Organic & Biomolecular Chemistry

RSC Publishing

PAPER

View Article Online
View Journal | View Issue

Cite this: *Org. Biomol. Chem.*, 2013, **11**, 8395

Synthesis, kinetic studies and molecular modeling of novel tacrine dimers as cholinesterase inhibitors†

Roney Anderson Nascimento de Aquino,[a] Luzia Valentina Modolo,[b] Rosemeire Brondi Alves[a] and Ângelo de Fátima*[a]

Received 29th August 2013,
Accepted 18th October 2013

DOI: 10.1039/c3ob41762j

www.rsc.org/obc

This study presents the synthesis of 15 new tacrine dimers as well as the K_i and IC_{50} results, studies of the kinetic mechanism, and molecular docking analysis of the dimers in relation to the cholinesterases hAChE, hBChE, *Ee*AChE and eqBChE. In addition to spectroscopic characterization, X-ray structure determination was performed for two of the new compounds. These new dimers were found to be mixed nanomolar inhibitors of the evaluated targets with a broad and significant selectivity profile, and these properties are dependent on both the type of the linker and the volume of the hydroacridine alicyclic ring. The results indicate that the aromatic linkers play a significant role in generating specific interactions with the half-gorge region of the catalytic center. Thus, these types of linkers can positively modulate the electronic properties of the tacrine dimers studied with an improvement of their cholinesterase inhibition activity.

Introduction

The hydrolases, including acetylcholinesterase (AChE, EC 3.1.1.7) and butyrylcholinesterase (BChE, EC 3.1.1.8), are important and widely distributed enzymes. AChE functions primarily as a regulatory enzyme at cholinergic synapses, whereas BChE acts as a nonspecific esterase for a range of substrates, such as anesthetics and narcotics, which are of particular interest.[1,2] These enzymes have received particular attention because they are targets in Alzheimer's disease (AD) therapy. Accordingly, inhibition of these two enzymes, selectively or non-selectively, is the predominant approach adopted in AD therapy.[3–5] In addition to reducing and improving poor psychiatric conditions in Alzheimer's patients, such as apathy and visual hallucinations,[6] cholinesterase inhibitors (ChEIs) have demonstrated significant therapeutic results in other cognitive disorders, such as Parkinson's disease, Lewy body dementia, vascular dementia, traumatic brain injury and cognitive disorders that occur in multiple sclerosis.[7–12] ChEIs have been able to eliminate the effects caused by addictive drugs and may be used as co-drugs for treatment of addicts.[13] Furthermore, ChEIs have been used in the treatment of glaucoma and myasthenia gravis and as competitors for cholinesterase sites in the case of poisoning by phosphate compounds.[14] Moreover, the development of ChEIs is important in the investigation of the mechanism of cholinergic transmission disorders.[15,16]

Recently, the results of pharmaceutical tests have indicated that ChEIs act *via* multiple pathways of neuronal protection on different targets.[17] Accordingly, favorable inhibitory activities have been observed for the following types of receptors/enzymes: *N*-methyl D-aspartate (NMDA), gamma-aminobutyric acid (GABA), the L-type voltage-dependent calcium channel (L-VDCC), nitric oxide synthase (NOS), and β- and γ-secretase.[18] In addition, ChEIs operate by inducing the activity of protein kinase type C (PKC) and consequently α-secretase, resulting in the reduction of harmful amyloid species levels.[18] Thus, ChEIs act as ligands directed to multiple targets that are suitable for treating multifactorial diseases, such as AD.[19]

Tacrine (1,2,3,4-tetrahydroacridin-9-amine, THA) is one of the oldest and most important ChEIs.[20–22] THA was the first drug approved by the FDA for the treatment of AD.[23] Although THA is a simple molecule to synthesize, it has been rarely used because of its hepatotoxic effects.[24,25] To improve its pharmacological profile, several molecular modification strategies have been adopted.[26,27] In 1996, Pang *et al.* synthesized a THA dimer (Fig. 1) that showed significant higher inhibitory potential for AChE than that shown by THA.[28] Moreover, this derivative has shown anti-amyloidogenic activity.[17,29] Amyloid deposits appear to play significant role in the etiology of AD.[30–34] As confirmed by X-ray data, when the dimer binds to

[a]*Grupo de Estudos em Química Orgânica e Biológica (GEQOB), Departamento de Química, ICEx, Universidade Federal de Minas Gerais, Belo Horizonte, MG 31270-901, Brazil. E-mail: adefatima@qui.ufmg.br; Fax: +55-31-3409-5700; Tel: +55-31-3409-6373*

[b]*Grupo de Estudos em Bioquímica de Plantas (GEBioPlan), Departamento de Botânica, ICB, Universidade Federal de Minas Gerais, Belo Horizonte, MG 31270-901, Brazil*

†CCDC 945409 and 945410. For crystallographic data in CIF or other electronic format see DOI: 10.1039/c3ob41762j

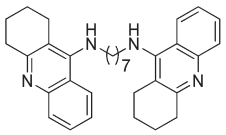

Fig. 1 Bis(7)THA: a tacrine dimer.

its target, it positions a THA component in the region known as the catalytic anionic site (CAS) close to the enzyme catalytic triad, while the other THA component is positioned at the entrance of the catalytic gorge, which is defined as the peripheral anionic site (PAS).[35] The PAS is responsible for the AChE molecular chaperone effect in the conversion of non-amyloidogenic molecules to amyloidogenic ones.[36,37]

An important feature of the dimers relates to the chemical nature of the linker used between the hydroacridine units.[26] Increased potency and specificity have been observed by exploiting specific interactions between the linker and the middle region of the cholinesterase catalytic gorge.[38]

To date, few studies with THA dimers have examined the effect that the variation of the nature of the aromatic linker has on the inhibition potency and the kinetic mechanism. Considering the importance of this class of substances, we have synthesized a series of 15 new tacrine dimers, which were evaluated kinetically and by molecular docking, to elucidate the underlying molecular phenomena and to aid in the development of new molecules and computational models.[39,40]

Results and discussion

The synthetic routes and the resultant dimers obtained in this study are summarized in Scheme 1.

The synthetic intermediates, chlorine–hydroacridine compounds (**5–7**), were obtained by the Friedlander condensation reaction in the presence of $POCl_3$, according to the procedure described in the literature.[41] As shown in Scheme 1, ketones **2–4** differ in the number of carbons in the alicyclic ring. This variation in the size of the alicyclic ring was used to evaluate the effect of the volume of the hydrophobic region on the inhibitory potential of the dimer. The available information on weak intermolecular interactions and their role in the binding of bioligands is limited.[42–44] Dimers were produced from the nucleophilic aromatic substitution reaction between compounds **5–7** and the diamines corresponding to the linkers (**8–13**), according to the procedure described in the literature.[45]

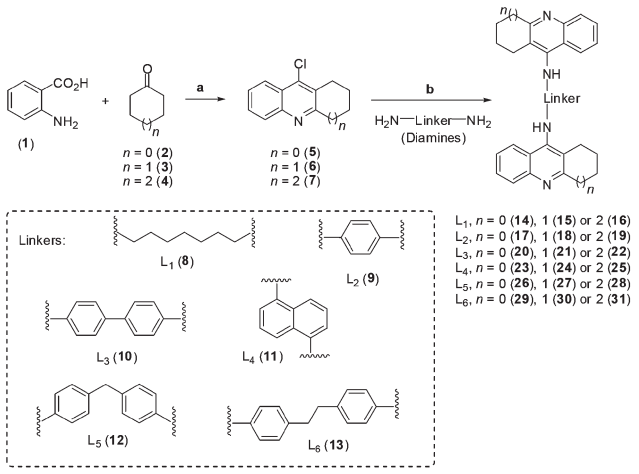

Scheme 1 Synthesis of THA analogues. *Reagents and conditions*: (a) for **5**: $POCl_3$, 120 °C, 2 h and for **6** and **7**: toluene, 160 °C, 2 h and then $POCl_3$, 120 °C, 2 h; (b) pentan-1-ol, reflux, 40 h.

Inhibition kinetics

The analysis of the overlapping double reciprocal plots at different inhibitor concentrations shows that the molecules synthesized in this study are mixed inhibitors of AChE and BChE.[46] These results suggest that although dimers occupy a significant fraction of the catalytic gorge, they do not compete for the same binding site as the substrate, in contrast to the inhibitor edrophonium, for example, which is positioned in intimate contact with the catalytic serine residue.[47] These observations are consistent with the X-ray structures of dual inhibitor complexes and with the results obtained from molecular modeling.[28,35,38,48] The literature shows that although there are representatives of the three types of kinetic mechanisms among cationic cholinesterase inhibitors, most are mixed mechanisms.[49]

The dissociation constants (K_i) for the compounds evaluated with respect to cholinesterase were obtained by the slope method[50] and are shown in Table 1. The K_i values obtained for the reference compounds, THA monomer and dimer **15**, are consistent with those previously published.[28,38] Compound **15** was found to be the most potent AChEI. This increased inhibitory potency is attributed to the ability of this molecule to optimally establish specific interactions in the CAS/PAS, especially in AChE.[28,35] An optimal distance exists between the hydroacridine components of the dimers and is suitable for simultaneous interaction with the CAS/PAS. Accordingly, dimers bearing n = 1 and aromatic linkers, such as the novel compounds **21** and **27**, were more potent than THA in the inhibition of hAChE. The distance between THA cores in both new THA dimers is similar to that of compound **15**.[28,45] The graph of the inhibitory potency of the dimers *versus* the distance between the two pyridine nitrogens shows a higher concentration of lower K_i values between 14.5 and 16 Å. This effect applies more to AChE. Nevertheless, there are compounds with nanomolar inhibitory potential for all types of linkers used, suggesting that the position of the specific receptor interaction sites is flexible.[45,51] This characteristic was also suggested by dynamic measurements of fluorescence titration.[52]

Part of the inhibitory potency of ChEIs, such as galantamine and THA, are attributed to their structural rigidity because there is only a small entropic loss associated with binding.[53] Despite the energy gain during the entropic bonding process due to the rigidity of the dimers with aromatic linkers, this energy gain does not overcome the reduced

Table 1 Inhibition constants (K_i) for THA dimers toward cholinesterases

	$K_i \pm$ SD (nM)				Selectivity	
Compound	hAChE	hBChE	*Ee*AChE	eqBChE	hAChE[a]	hBChE[b]
THA	23.2 ± 3.04	2.78 ± 0.15	18.3 ± 5.14	2.71 ± 0.46	0.12	8.35
14	6.43 ± 1.27	124 ± 43.9	28.0 ± 12.9	202 ± 158	19.3	0.05
15	1.12 ± 0.07	40.5 ± 7.66	0.61 ± 0.21	20.4 ± 4.60	36.2	0.03
16	1.20 ± 0.07	3.14 ± 2.48	1.01 ± 0.77	11.0 ± 0.90	2.62	0.38
17	106 ± 6.43	78.4 ± 37.6	109 ± 13.7	419 ± 90.6	0.74	1.35
18	19.8 ± 1.68	61.9 ± 25.9	51.0 ± 1.29	345 ± 192	3.12	0.32
19	728 ± 43.2	33.4 ± 13.9	265 ± 43.2	22.5 ± 7.50	0.05	21.8
20	6.93 ± 1.08	35.7 ± 3.59	83.1 ± 11.0	53.2 ± 7.28	5.15	0.19
21	2.67 ± 0.21	117 ± 36.2	10.0 ± 1.55	27.1 ± 9.23	43.8	0.02
22	31.0 ± 0.16	92.7 ± 9.03	22.1 ± 9.68	977 ± 59.5	2.99	0.33
23	397 ± 82.6	31.9 ± 1.07	96.1 ± 17.6	324 ± 64.6	0.08	12.5
24	395 ± 98.6	16.2 ± 2.27	111 ± 21.7	274 ± 12.6	0.04	24.4
25	1190 ± 44.8	31.6 ± 0.95	131 ± 40.6	91.8 ± 6.79	0.03	37.7
26	13.2 ± 3.37	148 ± 12.3	39.4 ± 8.66	117 ± 46.6	11.2	0.09
27	3.18 ± 0.77	22.2 ± 2.60	31.4 ± 6.45	40.8 ± 16.5	6.98	0.14
28	233 ± 86.7	658 ± 1.26	190 ± 62.0	1170 ± 49.7	2.82	0.35
29	15.9 ± 6.23	68.3 ± 1.09	37.7 ± 8.19	244 ± 2.66	4.30	0.23
30	30.8 ± 2.99	20.0 ± 1.80	5.13 ± 0.37	122 ± 25.5	0.65	1.54
31	1540 ± 82.6	95.3 ± 25.5	30.0 ± 5.59	563 ± 40.6	0.06	16.2

K_i is the mean of at least three independent experiments; SD, standard deviation; hAChE, human acetylcholinesterase; hBChE, human butyrylcholinesterase; *Ee*AChE, *Electrophorus electricus* acetylcholinesterase; eqBChE, equine butyrylcholinesterase. [a] $K_{i(hBChE)}/K_{i(hAChE)}$. [b] $K_{i(hAChE)}/K_{i(hBChE)}$.

ability of these ligands to adjust their components for optimal interactions with the appropriate areas of the target, as it occurs with compound **15**.

Although there is flexibility in the distance between the target interaction points,[45] the presence of rigid linker groups makes difficult the adjustment of the inhibitor molecule, and even if binding occurs, structural changes in the enzyme may occur simultaneously, resulting in significant energy cost.[35]

However, the aromatic linker leads to a significant reduction in the pK_{aH} value of the pyridine nitrogen. Lower values of pK_{aH} for the THA congener series result in lower potential for inhibition of AChE. This result is consistent with the direct contribution of a hydrogen bond involving the THA pyridine nitrogen and the carbonyl group of residue H440 of the target.[54,55] The possible ionic interaction involving residue E199 and the positive charge of the synthesized ligands is disfavored as also shown elsewhere.[56,57] The interactions with H440 and E199 have no equivalent in the PAS.[35] Furthermore, the suppression of the pyridine nitrogen charge reduces the effect of the cation–pi interaction between W84 and F330.[58] At pH 7.0, it was estimated that 97.5% of compound **15** is biprotonated (**15b**) (2.5% is the monoprotonated form) *versus* 85.5% of compound **21** (14.0% is monoprotonated). However, at pH 8.0 (in the same set of experiments), 79.5% of compound **15** was found to be biprotonated (20.0% was monoprotonated) while 30.5% of **21** was biprotonated (49.5% was monoprotonated). These results indicate the negative influence of electronic factors on the inhibitory potential of dimers with aromatic linkers. To confirm this hypothesis, we performed a study of the inhibition at pH 7.2 for compound **21** in relation to *Ee*AChE. The estimated proportions of the charged species of **21** were similar to those of **15** at pH 8.0. Also, the K_i value for *Ee*AChE obtained for **21** at pH 7.2 (11.0 ± 1.0 nM) was similar to that obtained at pH 8.0 (K_i = 10.0 ± 1.55 nM). These results suggest that the dual inhibitory activity of ChEI depends on the protonation of one of the nitrogens to be accommodated in the CAS gorge region. The X-ray data show that replacement of an amine nitrogen atom of the THA dimer with a sulfur atom results in a deprotonation of one pyridine nitrogen which in turn will compromise the binding to the CAS.[59] Butini and colleagues synthesized a biprotonatable THA dimer with a benzene linker separated by an ethylene group that is connected to the amine nitrogen of THA, which showed a K_i of 1.63 ± 0.29 nM (hAChE).[38] This value is similar to that obtained for **21** (K_i = 2.67 ± 0.21 nM; hAChE). However, the presence of a protonated THA unit in the ligand appears to be essential for inhibitory activity. Among the dimeric cholinesterase inhibitors with aromatic linkers already reported, the most potent ones have at least one THA unit.[38,60] In contrast, compounds that do not have a THA unit have a lower inhibitory potential, such as stilbamidine[15] and gallamine,[68] even though these compounds are dimeric cationic divalent inhibitors. The use of aromatic linkers that allow for pK_a reduction has been shown to be advantageous because it favors mobility across the blood–brain barrier.[15,54]

In general, by comparing the K_i values for both AChEs (Table 1), it is noted that the smaller the volume of the ligand is, the higher is the dimer potency on the human enzyme. The overlay of the X-ray structures of these molecules shows that for both AChEs, the catalytic gorge is essentially the same in terms of the residues participating in the enzyme mechanism.[61,62] Nevertheless, certain differences may explain the differential inhibitory profile of the dimers. The cluster involving residues V294 (acyl loop), A343 (helix 14) and V365 (helix

15) in hAChE is replaced by I294, V343 and I365, respectively, in *Ee*AChE. In the latter cluster, the corresponding residues have larger hydrophobic groups, which generate a distinct interaction effect. At the base of the Y124 loop (PAS), the S128 hAChE residue is replaced by A128 in *Ee*AChE. In the former case, the hydroxyl of S128 establishes a hydrogen bond with the side chain amide carbonyl of residue N150 (2.7 Å) and the side chain amide nitrogen of N100 (3.0 Å). This hydrogen bonding could lead to increased stability and less adaptability by the hAChE Y124 loop (PAS) in relation to the dimers, resulting in the lower potency of bulkier dimers.[48] Finally, in the outer portion of the alleged backdoor region, the hAChE R463 residue is replaced by L463 in *Ee*AChE.[63–65] This replacement can result in the increased stability/lower adaptability of the catalytic gorge loops of hAChE given the possible electrostatic interactions of R463 with residues E81 (Ω loop) and D131 (loop Y124/PAS). The increased potency of THA and huprine X in inhibiting *Tc*AChE is attributed to more favorable stacking of the ligand with F330, which replaces the Y337 residue in hAChE.[66] This analysis does not apply to *Ee*AChE because this residue exchange does not occur. However, a comparison between the X-ray structures of *Tc*AChE and *Ee*AChE shows that these structures are similar to each other with regard to the points mentioned above and may justify the difference in inhibition of hAChE and *Ee*AChE.[62,67]

The results in Table 1 reveal that THA is basically the most potent BChEI. This behavior is different from that observed for AChE. Although the interaction of the synthesized dimers with the surface of the target is greater than that of THA itself, this interaction does not appear to generate a set of specific interactions that can sufficiently compensate for the entropic loss of binding molecules.[43] However, the increased aromatic character of the ligand in the dimers is penalized by the reduced number of aromatic residues in the gorge of BChE, from **14** in AChE to **8** in BChE.[38,68] Finally, the introduction of a linker reduces the potential interaction between the amine nitrogen of THA and water molecules, which provides a significant structural component, as well as those of the medium which together interact significantly with residues of the gorge.[69,70]

The dimers with aromatic linkers showed significant inhibition for hBChE, especially compound **24** (K_i = 16.2 nM). The inhibition at nanomolar concentration observed in these cases is suggestive of the ability of these ligands to engage in specific interactions with the catalytic gorge of the enzyme.[38] Dimers **19**, **23–25** and **31** are more selective for hBChE in comparison with hAChE. The greatest gains of inhibitory potency for hAChE over hBChE occur with dimers **23–25** and to a lesser extent with dimers **17** and **18**. Among the evaluated compounds, these dimers possess less flexible linkers. These observations are consistent with the fact that the catalytic gorge of BChE has more available space than AChE, which allows the accommodation of molecules that are bulkier and less flexible.[38,49,71] A comparison of the results of the inhibitory potency relative to hBChE for compounds **15**, **21**, **27** and **30** and others of a similar nature described in the literature suggests that an optimum linker length exists for the inhibition of this enzyme.[38,71,72]

The strategy of increasing the number of carbons in the alicyclic rings to best fit the ligand-receptor has been successfully applied in developing bioligands.[64,73] Steinberg *et al.* observed that the expansion of "*n*" in hydroacridines (*n* = 0, 1 and 2) resulted in increased AChE inhibitory potency.[71] As shown in Table 1, the inhibitory effect of the number of methylene groups in the alicyclic ring on hAChE and, in certain cases, in *Ee*AChE resulted in the following order of potency: $n = 1 > n = 0 > n = 2$. In the case of the linear linker, the order of potency was $n = 1 > n = 2 > n = 0$. These results suggest that although the interactional subsites of the receptor have sufficient flexibility to accommodate an alicyclic ring with seven members, the most favorable connection depends on the flexibility of the linker used. Compounds with less flexible linkers showed higher relative potency if they had a compatible "*n*" value. Correa-Basurto *et al.* concluded that ligands with low volume would be more eligible to form pi–pi stacking interactions with *Tc*AChE CAS W84 residue.[74] The results showed that the rate of decrease in potency for the transition from *n* = 1 to *n* = 2 is greater for hAChE than for hBChE. This result may be a reflection of the increased available volume as well as the small role of the specific interactions in the hBChE catalytic gorge.[68] Tubocurarine, which is a bulk molecule, interacts with the CAS of the BChE as a peripheral AChEI, requiring higher concentrations for AChE inhibition.[75]

For BChE, the effect of varying the "*n*" value on the inhibitory potency depends on the type of linker and the enzyme used. The increase in the "*n*" value results in increased potency with a significant effect for dimers with linear linkers. This fact can be evaluated in terms of the largest space in the gorge of the BChE, with special emphasis on the region of the butyl pocket.[71,76] The substitution of alkyl linkers for aromatic linkers resulted, in general, in increased inhibitory potency for hBChE. For instance, with the exception of **26**, all aromatic dimers with *n* = 0 were more potent than **14**. As for the series with *n* = 1, compounds **24**, **27** and **30** were more potent than **15**. Thus, the use of aromatic linkers was shown to improve the potential of hBChE inhibition. On the other hand, the best inhibitors of eqBChE, except compounds **20** and **26** (series with *n* = 0), were those bearing an alkyl linker.

Table 1 shows the comparison of the two types of BChEs, which reveals that the dimers are generally more potent for hBChE. The overlap between the homology model for eqBChE (90.7% identity)[77–79] and the X-ray structure of hBChE[76] reveals four potentially significant differences in the region of the catalytic gorge. Three differences in the butyl loop exist where the residues G283, P285 and A277 in hBChE are replaced by D311, L313 and V305, respectively, in eqBChE. The other difference is the substitution of F398 in hBChE for I426 in eqBChE. The side chain of residue F398, which is directed toward the gorge lumen, is in close contact with residues W231 (butyl pocket) (3.6 Å) and H438 (catalytic triad) (3.3 Å). The acyl/butyl loop shows great mobility,[35,38] which suggests a functional role for this cholinesterase structural component.[38] The change in the

Table 2 Concentration (nM) of the THA dimers necessary to inhibit cholinesterases by 50% (IC_{50})

	IC_{50} ± SD (nM)				Selectivity	
Compound	hAChE	hBChE	*Ee*AChE	eqBChE	hAChE[a]	BChE[b]
THA	122 ± 7.46	47.3 ± 4.05	29.4 ± 3.60	4.33 ± 0.06	0.39	2.58
14	23.0 ± 3.32	246 ± 25.4	59.8 ± 8.07	179 ± 23.6	10.7	0.09
15	7.28 ± 0.69	141 ± 19.6	13.0 ± 0.33	64.3 ± 4.14	19.4	0.05
16	18.4 ± 1.60	39.9 ± 1.25	16.5 ± 1.21	28.3 ± 3.80	2.17	0.46
17	632 ± 68.7	452 ± 127	377 ± 28.4	608 ± 43.7	0.72	1.40
18	117 ± 25.4	267 ± 11.8	284 ± 57.0	186 ± 23.7	2.28	0.44
19	4720 ± 80.5	354 ± 154	3120 ± 211	169 ± 35.3	0.08	13.3
20	14.5 ± 3.40	1460 ± 192	685 ± 81.4	262 ± 1.74	101	0.01
21	54.8 ± 23.9	135 ± 8.90	69.5 ± 7.09	77.7 ± 10.7	2.46	0.41
22	15.1 ± 1.16	85.1 ± 26.5	562 ± 20.1	2110 ± 94.8	5.64	0.18
23	224 ± 14.4	165 ± 32.3	330 ± 51.0	315 ± 85.8	0.74	1.36
24	312 ± 37.2	329 ± 37.7	270 ± 9.68	157 ± 11.9	1.05	0.95
25	1080 ± 98.2	103 ± 24	1140 ± 406	153 ± 35.1	0.10	10.5
26	61.8 ± 4.61	109 ± 16.3	32.7 ± 9.97	63.5 ± 10.9	1.76	0.57
27	8.94 ± 0.42	206 ± 45.0	155 ± 8.40	113 ± 12.9	23.0	0.04
28	477 ± 66.2	1520 ± 133	2490 ± 532	201 ± 24.8	3.19	0.31
29	121 ± 0.35	15.1 ± 1.91	59.5 ± 9.56	65.9 ± 3.22	0.12	8.01
30	196 ± 2.31	40.3 ± 6.22	28.7 ± 8.82	87.7 ± 10.4	0.21	4.86
31	2850 ± 781	4870 ± 27.6	60.1 ± 22.3	2630 ± 108	1.71	0.59

IC_{50} is the mean of at least three independent experiments; SD, standard deviation; hAChE, human acetylcholinesterase; hBChE, human butyrylcholinesterase; *Ee*AChE, *Electrophorus electricus* acetylcholinesterase; eqBChE, equine butyrylcholinesterase. [a] $K_{i(hBChE)}/K_{i(hAChE)}$. [b] $K_{i(hAChE)}/K_{i(hBChE)}$.

behavior of the acyl/butyl loop observed in molecular dynamics simulations has been associated with the action of potent inhibitors.[48] In the eqBChE homology model, the side chain of residue L313 protrudes toward the lipophilic pocket formed by the residues F357, F385 and I384, which is a more intimate interaction than that of the P285 side chain in the same region for hBChE. In addition, residue D311 in eqBChE participates in a series of hydrogen bonds involving residues T312 (3.0 Å) and S315 (3.1 Å), which appears to confer stability on the butyl loop in eqBChE. Occupying the corresponding position in hBChE, the residue G283 does not establish specific interactions within the protein chain but confers higher structural flexibility on hBChE because it causes fewer steric effects.[80] Thus, the more flexible hBChE loop is more vulnerable to a change in its function caused by the presence of a dimeric inhibitor. Furthermore, the presence of a bulkier residue (V305) at the eqBChE catalytic gorge entrance may introduce an element of steric hindrance in the binding of THA dimers.[76]

Table 1 shows a comparison between the K_i values of a given compound against both AChEs with an average variation of 2.5 ± 1.2-fold from one enzyme to another. Regarding BChE, changes in potency occur on an average of 2.7 ± 1.1-fold. This result would suggest that, in terms of inhibitory potency, the findings obtained for certain ChEs could be extrapolated for human cholinesterases with relatively narrow limits of oscillation. However, certain synthesized compounds show a marked difference in their K_i values, *e.g.*, for AChE: **31** (51-fold), **20** (12-fold), **27** (10-fold) and **25** (9-fold) and for BChE: **24** (17-fold), **22** (11-fold), **23** (10-fold) and **18** (6-fold). Thus, our set of results clearly indicates that extrapolations in inhibitory activities of cholinesterases must be used with caution, particularly for AChE. Indeed, structural peculiarities of cholinesterases from different organisms appear to have a great effect on the inhibition of AChE as BChE are found to be more promiscuous.[38,68,71]

The IC_{50} values relative to cholinesterases were determined according to Korabecny *et al.*[81] and are shown in Table 2. A comparison between K_i and IC_{50} values shows that for a given linker, the relationships of inhibitory potency remain the same. However, some exceptions were found even with respect to selectivity.

Fig. 2 shows the schematic representation of equilibria reactions established among ChEs, their substrate and corresponding inhibitors.

To determine the degree to which the binding of an inhibitor changes the affinity of the enzyme for the substrate, we obtained experimentally the α values using Dixon's graphical method (Table 3).[82,83]

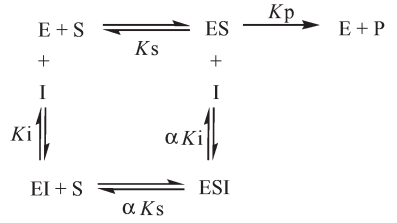

Fig. 2 Representation of equilibria reactions established in a medium containing a ChE, its substrate and a potential inhibitor (modified from Sussman *et al.*[89]). E, enzyme; S, substrate; K_s, constant for substrate dissociation; K_i, constant for inhibitor dissociation; α, apparent constant; K_p, constant related to the product formation.

Table 3 Alpha (α) values for THA and corresponding dimers against cholinesterases[a]

Compound	hAChE	hBChE	*Ee*AChE	EqBChE
THA	5.41	3.13	1.4	2.41
14	2.57	1.03	2.22	3.92
15	2.30	2.21	5.15	1.16
16	10.7	9.67	2.24	3.00
17	2.40	4.13	1.38	1.78
18	1.62	1.61	2.57	1.50
19	65.8	2.12	2.06	4.39
20	2.39	8.19	2.71	1.68
21	7.12	1.91	2.16	1.73
22	1.90	1.97	5.77	1.71
23	1.05	4.29	1.96	1.71
24	1.62	2.98	2.06	1.65
25	1.87	1.27	2.27	2.24
26	2.36	2.5	2.16	2.20
27	3.65	1.68	2.09	1.55
28	3.72	6.11	1.19	3.80
29	6.18	1.24	4.00	1.13
30	4.74	3.38	31.0	1.41
31	1.77	2.59	2.77	12.7

[a] hAChE, human acetylcholinesterase; hBChE, human butyrylcholinesterase; *Ee*AChE, *Electrophorus electricus* acetylcholinesterase; eqBChE, equine butyrylcholinesterase.

The α values were in the range of 2–10 and corroborate those previously described for THA and its derivatives.[55] Thus, the synthesized dimers still retain the high affinity of THA from which they originated. Dimers such as **23** in relation to hAChE (α = 1.05) and **14** relative to hBChE (α = 1.03) exhibit higher similar interactions with the corresponding inhibited ChE. In contrast, compound **19** relative to hChEs appears to present a distinct pattern of interaction with the enzymes.[84] This result may be explained by the decreased flexibility and increased volume of compound **19** and/or its greater competitiveness as evidenced by the experimental double reciprocal plot. The acetylation of the enzyme[84] could make difficult the accommodation of dimer **19** due to its volume.[55] Overall, the α values (Table 3) described here are in agreement with ChEIs that exhibit a mixed-type inhibition profile.[46] Among the enzymes investigated, *Ee*AChE has the lowest variation of α over a wide range of K_i values. The reduction, on average, of free energy necessary to bind the inhibitor to acetylated/butylated ChE is usually by 6%.[43] Our findings show that the highest values of free energy were as follows: hAChE (7.9%), hBChE (5.9%), *Ee*AChE (5.5%) and eqBChE (4.7%). Also, the increase in the K_i value suggests that the enzyme is experiencing steric/conformational changes during acetylation/butylation.[85] This also applies to K_s values.[85,86]

Molecular docking

The X-ray structure of the bis-7-THA:*Tc*AChE complex (PDB 2CKM) was used to estimate the conformation of dimers by molecular docking.[35,43] Yonetani–Theorell's kinetic analysis to define the grid revealed that the synthesized dimers bind to the catalytic gorge of *Ee*AChE. Fig. 3 shows the binding of compound **21** in the catalytic gorge of *Tc*AChE obtained by molecular docking.

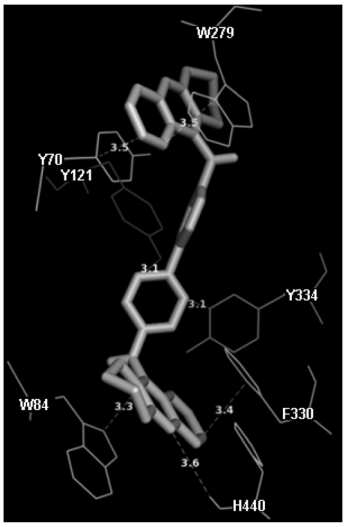

Fig. 3 Binding of compound **21** in the catalytic gorge of *Tc*AChE.

We found similar results from the molecular docking of other synthesized dimers into the activity site of AChE. Indeed, the competition between dimer **21** and THA for the catalytic site of *Ee*AChE observed experimentally (Tables 1 and 2) was confirmed by Yonetani–Theorell's kinetic analysis.[69,87,88]

The quinolinic cores of the dimer **21** establish two double pi–pi stacking interactions with residues W279 (3.5 Å) and Y70 (3.5 Å) (Fig. 3, upper side) and F330 (3.4 Å) and W84 (3.3 Å) (Fig. 3, lower side). The peptide carbonyl of H440 functions as a hydrogen bond acceptor of the protonated pyridine nitrogen present in **21** (3.6 Å). The residue H440 comprises the catalytic triad of this class of enzyme.[89] Additionally, Y121 can establish a hydrogen bond with the aromatic linker at a distance of 3.1 Å.

An inter-aromatic interaction is established between Y334 and the linker (3.1 Å). A similar arrangement was observed for other classes of ligands bearing a benzidine nucleus.[90]

Our molecular docking results with synthesized THA dimers are in agreement with those reported for other dimers.[38,59,69] The observed binding pattern is typical of ligands with an increased ability to affect ChE activity.[38] Therefore, structural elements that play an important role in the conformational/structural function/flexibility of the enzyme, such as SH_3-like structural domains,[91] have the ability to be altered/retained by the binding of the dimers. Thus, the position, organization, and retention of the aromatic residues Y70, Y121, and W279 (in the PAS) or W84, F330, and Y334 (in the CAS) comprise likely hot-spots,[92] whose loss of mobility impacts ChE activity. These interactions contribute significantly to the binding energy of the dimers that in turn result in ChE inhibition (Table 1). The docking results suggest that the search for inter-aromatic interactions between the linkers and the ChE mid-gorge (Fig. 3) is a good strategy for the design of better inhibitors. The best conformational results

were verified for compounds with a notorious ability to interact with both CAS/PAS and the half gorge region. In this sense, the linker length (*L*; Scheme 1) will confer multi-binding ability on the dimers. The experimental results support this idea (Tables 1 and 2).

The increase in the "*n*" value augments the dimer potency against BChE as this enzyme possesses a larger catalytic gorge. As for AChE, molecular docking shows that improved interactions occur for dimers with $n = 1$, similar to that observed for THA.

The interaction of the dimer with the half-gorge region shows that aromatic linkers are in closer contact with residues Y334 and Y121 (Fig. 3) than with aliphatic ones. These observations suggest that the projection of the aromatic linker toward the acyl pocket can be an important element in the bioligand design strategy for this target. Other studies also support this hypothesis.[28,38,55]

The arrangement of the positive charges of the ligand in relation to aromatic residues of the enzyme (Fig. 3) is typical of various dimeric cationic divalent cholinesterase inhibitors.[69] The minimum average distance observed for the synthesized dimers in relation to Oγ of S200 was 5.0 ± 0.5 Å. This is consistent with the minimum value of 4.5 ± 0.5 Å described for other mixed-type AChEIs[35,59,61,66,69] and higher than that of edrophonium (3.4 Å), a competitive AChEI.[47]

The homodimer **21** was found to be the most selective AChEI with the ratio K_i (hBChE)/K_i (hAChE) equal to 44 (Table 1).

The number of specific interactions established between **21** and hBChE (Fig. 4) is lower than that observed in the AChE catalytic gorge. The most significant interactions established were: (i) pi–pi stacking (3.7 Å) between the quinolinic portion of the ligand and the residue W82; (ii) inter-aromatic between the linker and the residue Y332 (3.7 Å) and (iii) those between the peptide carbonyl of H438 and the protonated pyridine nitrogen ligand (3.4 Å).

The absence of PAS in BChE[68,93] makes AChE more eligible as a target of synthesized dimers through the establishment of pi–pi stacking interactions. Nevertheless, it is suggested that Y332 in BChE compensates for the lack of PAS allowing for the formation of pi–pi type stack interactions.[94,95] From ITC measurements, Boehr *et al.* suggested that each pi–pi stacking interaction contributes with 2 kcal mol^{-1} to the binding energy.[96] Taking this into account, the pi–pi type stack interactions were the major contributors to the binding energy of synthesized dimers as attested by the K_i values (Table 1). These specific interactions have been used to design specific inhibitors for phosphotransferases[96] and AChE/BChE as well.[93]

This study shows a significant contribution of residues Y332 (pi–pi stacking) and D70 (hydrogen bonding) for the stabilization of the synthesized dimers in catalytic site of BChE. It is suggested that the interaction between dimeric ligands and this region competes with the formation of interactions between the ligand and the residue F278.[71] In the case of dimers with aromatic linkers, interactions with W84 would be favoured over those with D70–Y332 due to the loss, to some extent, of the pi–pi stacking interaction in the CAS.[94] Dual inhibitors bearing small linkers seem to be more efficient BChEIs due to the ability to better interact with Y332.[28,45] Interactions with W231, W430 and F329 also appear to be significant. Dimers **29–31**, which present longer linkers, are also able to interact with residues F278, I356 and Y282 (gorge entrance). Molecular docking results suggest that the THA unit of longer dimers interact in a face-to-edge fashion with F278. Indeed, F278 has been suggested as a possible peripheral site of interaction in BChE.[71] Also, residues I356 and Y282 comprise a small hydrophobic cluster in the AChE/BChE gorge entrance.[80,97]

Compound **16** was the most potent dimeric inhibitor of BChE among the THA dimers tested (Tables 1 and 2). Molecular docking analysis revealed that one acridine unit of **16** interacts with CAS while the other is oriented toward the flexible butyl pocket. Thus, the dimer **16** is completely inserted into the lower region of the BChE gorge. As previously suggested,[71] the increase in "*n*" improves the inhibitory activity of a due compound against BChE. Our results (Table 1), however, show that the increase of "*n*" value must be accompanied by an increase in the linker flexibility to guarantee an enhancement of ChEI performance.

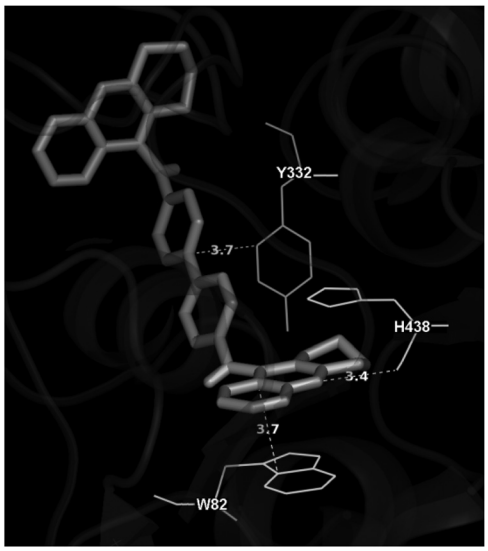

Fig. 4 Binding of compound **21** in the catalytic gorge of hBChE.

Conclusions

The THA dimeric derivatives used in this study act as mixed-type ChEIs independent of the nature and length of the linker. THA dimers bearing aromatic linkers establish specific interactions with the half-gorge of the cholinesterase studied. Therefore, the use of different aromatic linkers allows for obtaining inhibitors of particular selectivity toward AChE or BChE. Overall, the length, electronic features and flexibility of

the aromatic linker play a pivotal role in the design of more effective dual inhibitors of cholinesterases.

Experimental

General methods and materials

The substances used in this study (toluene, pentan-1-ol, compounds **1–4** and **8–13**, $POCl_3$, $NaHCO_3$, ethyl acetate, methanol, dichloromethane and trifluoroacetic acid) were purchased from Sigma-Aldrich and used without further treatment. The synthesis reactions and products were monitored by thin layer chromatography (TLC) (Polygram 0.20 mm MACHEREY-UV254 – NAGEL) under ultraviolet light (λ = 254 and 365 nm). Adsorption chromatography was performed using a column of silica gel (70–230 mesh and 230–400 mesh, from Aldrich). The melting temperatures were measured using a GEHAKA melting point PF1500 apparatus. The nuclear hydrogen magnetic resonance spectra (^{1}H NMR) and carbon nuclear magnetic resonance spectra (^{13}C NMR) were obtained at 200 MHz on a Bruker AVANCE DPX 200 spectrometer. For spectra at 400 MHz, a Nuclear Magnetic Resonance Bruker AVANCE DRX 400 spectrometer was used. The chemical shifts (δ) are expressed in parts per million (ppm) and are related to signals from tetramethylsilane (TMS) in the ^{1}H NMR spectra and by deuterated solvent in the ^{13}C NMR spectra. The multiplicity of the signals in the ^{1}H NMR spectra was indicated according to the following convention: s (singlet), d (doublet), t (triplet), qui (quintet), and m (multiplet). ^{1}H NMR data are presented in the following order: chemical shift in ppm (integration, multiplicity, coupling constant (J) in hertz (Hz), assignment). The characterization of the compounds by single-crystal X-ray analysis was performed at T = 150 K using a GEMINI 4-circles diffractometer with a CCD detector. The absorbance readings for the concentration–response curves and for the kinetic experiments were performed at 412 nm on a Thermo Scientific Multiskan® Spectrum microplate spectrophotometer managed by Thermo Scientific SkanIt Software. The elemental analysis was performed using a Perkin Elmer Series II – CHNS/O Analyser 2400. The HRMS measurements were performed using a Shimadzu Liquid Chromatograph with a High Resolution Mass Detector model LCMS-IT-TOF.

Synthesized compounds

9-Chloro-2,3-dihydro-1*H*-cyclopenta[*b*]quinoline (5). To a mixture of 2-aminobenzoic acid (8.22 g, 59.95 mmol) and cyclopentanone (6.07 g, 72.21 mmol) at 0 °C was added $POCl_3$ (50 mL). The resulting mixture was heated at 120 °C, magnetically stirred for 2 h and then cooled to room temperature. The reaction mixture was then slowly added to an aqueous solution of KOH (224 g in 400 mL of water) at 0 °C. The reaction mixture was extracted four times with 100 mL of CH_2Cl_2. The organic phase was dried with $MgSO_4$ and filtered, and the solvent was removed under vacuum. The product was purified using a flash silica column (eluent 10 : 4 : 0.1 hexane–ethyl acetate–triethylamine). Compound **5** was obtained as a light beige solid (3.36 g, 16.48 mmol, 28%), mp 85–87 °C. ^{1}H NMR (200 MHz, $CDCl_3$): δ = 7.98 (1H, d, $J_{4,3}$ 7.9), 7.89 (1H, d, $J_{5,6}$ 7.9), 7.53 (1H, t, $J_{4,5} = J_{5,6}$ 7.9), 7.39 (1H, t, $J_{3,4} = J_{5,4}$ 7.9), 3.07 (2H, t, $J_{10,9}$ 7.5), 2.98 (2H, t, $J_{10,11}$ 7.5), 2.08 (2H, qui, $J_{9,10} = J_{11,10}$ 7.5). ^{13}C NMR (50 MHz, $CDCl_3$): δ = 167.6, 148.6, 137.7, 134.1, 129.3, 129.0, 126.6, 125.4, 123.7, 35.7, 30.5, 22.9. Elemental analysis: calc. for $C_{12}H_{10}ClN$: C, 70.77; H, 4.95; N, 6.88; found: C, 71.15; H, 4.51; N, 7.14. HRMS (ESI) calc. for $C_{12}H_{10}ClN$ $[M + H]^+$: 204.0580, found: 204.0524.

9-Chloro-5,6,7,8-tetrahydroacridine (6). To a solution of 2-aminobenzoic acid (2.47 g, 17.98 mmol) in toluene (5 mL) was added cyclohexanone (2.14 g, 21.78 mmol). The resulting mixture was refluxed at 160 °C in a Dean–Stark apparatus with magnetic stirring for 2 h. The system was cooled to room temperature and maintained at 0 °C for 12 h. From 3.52 g (16.2 mmol) of the formed precipitate, 3.38 g (15.54 mmol) was slowly added to $POCl_3$ (10.01 g, 65.31 mmol) in a 25 mL flask. The resulting mixture was stirred and refluxed at 120 °C for 2 h. After this period, the mixture was cooled to room temperature and then added slowly to an aqueous solution of KOH (32.95 g KOH in 60 mL of water) in an ice bath with magnetic stirring. The reaction mixture was extracted four times with 100 mL of CH_2Cl_2. The organic phase was dried with $MgSO_4$. The organic solvent was removed and the product was purified using a flash silica column (eluent 10 : 0.1 chloroform–triethylamine). Compound **6** was obtained as a light yellow solid (8.3 g, 14 : 16 mmol, 80%), mp 65–67 °C. ^{1}H NMR (200 MHz, $CDCl_3$): δ = 8.10 (1H, d, $J_{4,3}$ 7.8), 7.96 (1H, d, $J_{5,6}$ 7.8), 7.63 (1H, t, $J_{4,5} = J_{6,5}$ 7.8), 7.48 (1H, t, $J_{3,4} = J_{5,4}$ 7.8), 3.15–2.90 (4H, m), 1.95–1.85 (4H, m). ^{13}C NMR (50 MHz, $CDCl_3$): δ = 159.6, 146.8, 141.7, 129.5, 129.0, 128.8, 126.7, 125.5, 123.9, 34.3, 27.7, 22.8. Elemental analysis: calc. for $C_{13}H_{12}ClN$: C, 71.72; H, 5.56; N, 6.43; found: C, 72.13; H, 5.62; N, 6.63. HRMS (ESI) calc. for $C_{13}H_{12}ClN$ $[M + H]^+$: 218.0737, found: 218.1100.

11-Chloro-7,8,9,10-tetrahydro-6*H*-cyclohepta[*b*]quinoline (7). This compound was obtained using the same procedure as that for compound **5**. The following quantities of reagents were used: 2.05 g (14.98 mmol) of 2-aminobenzoic acid, 1.69 g (15.08 mmol) of cycloheptanone, 20.56 g (134.1 mmol) of $POCl_3$, 56.13 g of KOH in 100 mL of water, and 60 mL of CH_2Cl_2. Compound **7** was obtained as a brown solid (0.54 g, 2.31 mmol, 16%), mp 91–93 °C. ^{1}H NMR (200 MHz, $CDCl_3$): 7.94 (1H, d, $J_{4,3}$ 7.6), 7.83 (1H, d, $J_{5,6}$ 7.6), 7.46 (1H, t, $J_{4,5} = J_{5,6}$ 7.6), 7.33 (1H, t, $J_{3,4} = J_{5,4}$ 7.6), 3.16–2.86 (4H, m), 1.85–1.37 (6H, m). ^{13}C NMR (50 MHz, $CDCl_3$): 164.7, 146.4, 139.7, 133.8, 129.1, 128.9, 126.7, 125.4, 124.5, 40.2, 31.9, 30.4, 27.5, 26.9. Elemental analysis: calc. for $C_{14}H_{14}ClN$: C, 72.57; H, 6.09; N, 6.04; found: C, 72.90; H, 6.32; N, 6.84. HRMS (ESI) calc. for $C_{14}H_{14}ClN$ $[M + H]^+$: 232.0893, found: 232.0810.

***N*-(7-(2,3-Dihydro-1*H*-cyclopenta[*b*]quinolin-9-ylamino)heptyl)-2,3-dihydro-1*H*-cyclopenta[*b*]quinolin-9-amine (14).** Compound **5** (228.6 mg, 1.12 mmol) was added to a solution containing 72.6 mg (0.56 mmol) of compound **8** in 1.5 mL of pentan-1-ol. The mixture was refluxed for 40 h. The system was then cooled to room temperature and 30 mL of 2 M HCl was added. The

system remained under stirring at 40 °C for 2 h. The resulting precipitate was filtered and washed with 2 mL of each of the following solvents: water, toluene and hexane. The product was recrystallized from a mixture of trifluoroacetic acid (TFA)–water to produce a gray solid (405.3 mg, 0.448 mmol, 79%), which decomposes at 333 °C. ^{1}H NMR (400 MHz, CD_3OD): 8.31 (2H, d, $J_{3,2}$ 7.8), 7.82 (2H, t, $J_{3,4} = J_{5,4}$ 7.8), 7.71 (2H, d, $J_{4,5}$ 7.8), 7.60 (2H, t, $J_{2,3} = J_{4,3}$ 7.8), 3.79 (4H, t, $J_{14,13}$ 7.5), 3.36 (4H, t, $J_{9,8}$ 7.5), 3.16 (4H, t, $J_{9,10}$ 7.5), 2.26 (4H, qui, $J_{10,9} = J_{8,9}$ 7.5), 1.79–1.70 (4H, m), 1.52–1.41 (6H, m). ^{13}C NMR (100 MHz, CD_3OD): 155.7, 139.9, 134.7, 128.3, 124.7, 121.4, 119.3, 112.3, 46.8, 33.5, 33.4, 33.2, 31.0, 28.5, 24.6. Elemental analysis: calc. for $C_{31}H_{36}N_4 \cdot 3C_2HO_2F_3 \cdot H_2O$: C, 53.88; H, 5.01; N, 6.79; found: C, 54.09; H, 5.23; N, 7.26. HRMS (ESI) calc. for $C_{31}H_{36}N_4$ $[M + H]^+$: 465.3018, found: 465.3182.

***N*-(7-(5,6,7,8-Tetrahydroacridin-9-ylamino)heptyl)-5,6,7,8-tetrahydroacridin-9-amine (15).** This compound was obtained using the same procedure as that for compound **14**. The following quantities of the reagents were used: 206.9 mg (0.95 mmol) of compound **6** and 61.5 mg (0.47 mmol) of compound **8**. However, recrystallization occurred from a methanol–2 M HCl solution, from which compound **15** was obtained as a pale green solid (221.6 mg, 0.39 mmol, 83%), mp 146–156 °C. ^{1}H NMR (400 MHz, CD_3OD): 8.38 (2H, d, $J_{3,2}$ 7.9), 7.84 (2H, t, $J_{3,4} = J_{5,4}$ 7.9), 7.77 (2H, d, $J_{4,5}$ 7.9), 7.57 (2H, t, $J_{2,3} = J_{4,3}$ 7.9), 3.95 (4H, t, $J_{15,14}$ 7.0), 3.01 (4H, t, $J_{9,8}$ 5.2), 2.72–2.65 (4H, m), 2.03–1.78 (12H, m), 1.52–1.41 (6H, m). ^{13}C NMR (100 MHz, CD_3OD): 158.9, 152.6, 140.6, 135.0, 127.3, 127.2, 121.0, 117.9, 113.7, 32.4, 30.8, 30.2, 28.5, 25.8, 23.9, 22.7. Elemental analysis: calc. for $C_{33}H_{40}N_4 \cdot 4HCl$: C, 62.07; H, 6.95; N, 8.77; found: C, 62.06; H, 6.99; N, 8.54. HRMS (ESI) calc. for $C_{33}H_{40}N_4$ $[M + H]^+$: 494.3331, found: 494.2961.

***N*-(7-(7,8,9,10-Tetrahydro-6*H*-cyclohepta[*b*]quinolin-11-ylamino)heptyl)-7,8,9,10-tetrahydro-6*H*-cyclohepta[*b*]quinolin-11-amine (16).** This compound was obtained using the same procedure as that for compound **14**. The following quantities of reagents were used: 223.0 mg (0.96 mmol) of compound **7** and 62.2 mg (0.48 mmol) of compound **8**. Compound **16** was obtained as an orange solid (286.0 mg, 0.29 mmol, 61%), mp 160–165 °C. ^{1}H NMR (400 MHz, CD_3OD): 8.33 (2H, d, $J_{3,2}$ 7.8), 7.85 (2H, t, $J_{3,4} = J_{5,4}$ 7.8), 7.79 (2H, d, $J_{4,5}$ 7.8), 7.61 (2H, t, $J_{2,3} = J_{4,3}$ 7.8), 3.78 (4H, t, $J_{16,15}$ 7.8), 3.17 (4H, t, $J_{9,8}$ 5.5), 2.98 (4H, t, $J_{11,12}$ 5.3), 2.00–1.90 (4H, m), 1.90–1.70 (12H, m), 1.44–1.37 (6H, m). ^{13}C NMR (100 MHz, CD_3OD): 160.5, 158.7, 139.5, 134.7, 128.1, 126.2, 121.3, 119.5, 118.7, 36.0, 33.0, 32.5, 30.8, 28.8, 28.6, 28.4, 27.7. Elemental analysis: calc. for $C_{35}H_{44}N_4 \cdot 4C_2HO_2F_3$: C, 52.87; H, 4.95; N, 5.74; found: C, 53.83; H, 4.52; N, 6.42. HRMS (ESI) calc. for $C_{35}H_{44}N_4$ $[M + H]^+$: 521.3644, found: 521.3404.

***N*^{1},*N*^{4}-Bis(2,3-dihydro-1*H*-cyclopenta[*b*]quinolin-9-yl)benzene-1,4-diamine (17).** This compound was obtained using the same procedure as that for compound **14**. The following quantities of reagents were used: 231.1 mg (1.13 mmol) of compound **5** and 61.5 mg (0.52 mmol) of compound **9**. Compound **17** was obtained as a brown solid (359.8 mg, 0.4 mmol, 77%), mp >360 °C. ^{1}H NMR (400 MHz, CD_3OD): 8.46 (2H, d, $J_{6,5}$ 7.8), 7.96 (2H, t, $J_{8,7} = J_{6,7}$ 7.8), 7.89 (2H, d, $J_{5,6}$ 7.8), 7.74 (2H, t, $J_{5,6} = J_{7,6}$ 7.8), 7.44 (4H, s), 3.25 (4H, t, $J_{12,11}$ 7.5), 2.52 (4H, t, $J_{12,13}$ 7.5), 2.23–2.11 (4H, m). ^{13}C NMR (100 MHz, CD_3OD): 165.0, 153.5, 140.4, 139.9, 135.1, 129.0, 128.6, 125.5, 121.7, 120.6, 119.2, 33.8, 33.7, 25.0. Elemental analysis: calc. for $C_{30}H_{26}N_4 \cdot 2C_2HO_2F_3$, C, 60.9; H, 4.21; N, 8.35; found: C, 61.39; H, 3.52; N, 8.75. HRMS (ESI) calc. for $C_{30}H_{26}N_4$ $[M + H]^+$: 443.2236, found: 443.2278.

***N*^{1},*N*^{4}-Bis(5,6,7,8-tetrahydroacridin-9-yl)benzene-1,4-diamine (18).** This compound was obtained using the same procedure as that for compound **14**. The following quantities of reagents were used: 232.1 mg (1.07 mmol) of compound **6** and 57.4 mg (0.53 mmol) of compound **9**. Compound **18** was obtained as a brown solid (363.5 mg, 0.39 mmol, 74%), mp >360 °C. ^{1}H NMR (200 MHz, CF_3CO_2D): 7.83–7.60 (6H, m), 7.35 (2H, t, $J_{7,6} = J_{5,6}$ 6.8), 7.16 (4H, s), 3.14–2.89 (4H, m), 2.75–2.58 (4H, m), 2.06–1.86 (8H, m). ^{13}C NMR (50 MHz, CF_3CO_2D): 156.5, 155.8, 141.4, 140.4, 136.3, 128.8, 127.7, 127.2, 121.6, 119.5, 118.3, 31.0, 26.3, 23.5, 22.5. Elemental analysis: calc. for $C_{32}H_{30}N_4 \cdot 2C_2HO_2F_3$: C, 61.89; H, 4.62; N, 8.02; found: C, 62.05; H, 3.93; N, 8.45. HRMS (ESI) calc. for $C_{32}H_{30}N_4$ $[M + H]^+$: 471.2549, found: 471.2430. X-ray crystallography: $C_{32}H_{30}N_4$, triclinic, $P\bar{1}$, a = 8.7040(3) Å, b = 10.8569(3) Å, c = 11.5890(3) Å, α = 100.578(3), β = 103.072(3), γ = 96.793(3), v = 1033.93 Å^3, Z: 1 Z': 0, R = 5.41. ORTEP representation is shown in Fig. 5.

***N*^{1},*N*^{4}-Bis(7,8,9,10-tetrahydro-6*H*-cyclohepta[*b*]quinolin-11-yl)-benzene-1,4-diamine (19).** This compound was obtained using the same procedure as that for compound **14**. The following quantities of reagents were used: 233.8 mg (1.0 mmol) of compound **7** and 54.66 mg (0.5 mmol) of compound **9**. Compound **19** was obtained as an orange solid (405.8 mg, 0.43 mmol, 85%), mp 255–260 °C. ^{1}H NMR (400 MHz, CD_3OD): 8.18 (2H, d, $J_{6,5}$ 8.7), 7.96–7.89 (4H, m), 7.65–7.59 (2H, m), 7.18 (4H, s), 3.28 (4H, m), 2.90 (4H, t, $J_{15,14}$ = 8.0), 1.95–1.89 (8H, m), 1.67–1.59 (4H, m). ^{13}C NMR (100 MHz, CD_3OD): 163.2, 155.0, 141.8, 139.7, 135.1, 129.1, 126.7, 125.2, 125.0, 121.7, 36.6, 33.1, 29.4, 28.5, 27.7. Elemental analysis: calc. for $C_{34}H_{34}N_4 \cdot 2C_2HO_2F_3 \cdot H_2O$: C, 61.29; H, 5.14; N, 7.52; found: C, 61.38; H, 4.0; N, 7.76. HRMS (ESI) calc. for $C_{34}H_{34}N_4$ $[M + H]^+$: 499.2862, found: 499.2886.

***N*-{4-[4-({1*H*,2*H*,3*H*-Cyclopenta[*b*]quinolin-9-yl}amino)phenyl]-phenyl}-1*H*,2*H*,3*H*-cyclopenta[*b*]quinolin-9-amine (20).** This compound was obtained using the same procedure as that for

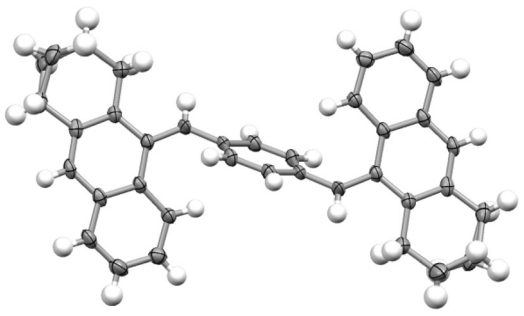

Fig. 5 ORTEP representation of the X-ray crystal structure of compound **18**. The displacement of the ellipsoids is drawn at 50% probability.

compound **14**. The following quantities of reagents were used: 262.6 mg (1.29 mmol) of compound **5** and 124.2 mg (0.67 mmol) of compound **10**. Compound **20** was obtained as a light yellow solid (515.9 mg, 0.53 mmol, 79%), mp 252–256 °C. ^{1}H NMR (400 MHz, CD_3OD): 8.47 (2H, d, $J_{8,7}$ 7.8), 7.96 (2H, t, $J_{10,9} = J_{8,9}$ 7.8), 7.88 (2H, d, $J_{9,10}$ 7.8), 7.84 (4H, d, $J_{3,2}$ 8.5), 7.74 (2H, t, $J_{7,8} = J_{9,8}$ 7.8), 7.44 (4H, d, $J_{2,3}$ 8.5), 3.23 (4H, t, $J_{14,13}$ 7.5), 2.49 (4H, t, $J_{14,15}$ 7.5), 2.14 (4H, qui, $J_{15,14} = J_{13,14}$ 7.5). ^{13}C NMR (100 MHz, CD_3OD): 164.8, 153.5, 140.9, 140.6, 140.4, 135.0, 129.4, 129.0, 128.5, 125.5, 121.7, 119.2, 112.3, 33.7, 33.6, 25.0. Elemental analysis: calc. for $C_{36}H_{30}N_4{\cdot}2C_2HO_2F_3{\cdot}3H_2O$: C, 60.0; H, 4.78; N, 7.0; found: C, 60.25; H, 3.09; N, 7.03. HRMS (ESI) calc. for $C_{36}H_{30}N_4$ $[M + H]^+$: 519.2549, found: 519.2311.

***N*-(4-{4-[(1,2,3,4-Tetrahydroacridin-9-yl)amino]phenyl}phenyl)-1,2,3,4-tetrahydroacridin-9-amine (21).** This compound was obtained using the same procedure as that for compound **14**. The following quantities were used: 266.0 mg (1.22 mmol) of compound **6** and 108.8 mg (0.59 mmol) of compound **10**. Compound **21** was obtained as an orange solid (579.8 mg, 0.58 mmol, 98%), mp 186–192 °C. ^{1}H NMR (400 MHz, CD_3OD): 8.00 (2H, d, $J_{8,7}$ 8.7), 7.90–7.83 (4H, m), 7.75 (4H, d, $J_{3,2}$ 8.7), 7.52–7.44 (2H, m), 7.29 (4H, d, $J_{2,3}$ 8.6), 3.18 (4H, t, $J_{14,13}$ 6.3), 2.65 (4H, t, $J_{15,16}$ 6.1), 2.05–1.97 (4H, m), 1.97–1.87 (4H, m). ^{13}C NMR (100 MHz, CD_3OD): 155.2, 142.2, 139.6, 139.1, 134.5, 129.0, 127.3, 126.5, 125.3, 120.6, 119.5, 117.9, 111.6, 29.8, 26.5, 23.0, 22.0. Elemental analysis: calc. for $C_{38}H_{34}N_4{\cdot}4C_2HO_2F_3$: C, 55.1; H, 3.82; N, 5.59; found: C, 55.6; H, 2.83; N, 5.69. HRMS (ESI) calc. for $C_{38}H_{34}N_4$ $[M + H]^+$: 547.2862, found: 547.3013. X-ray crystallography: $C_{38}H_{34}N_4$, triclinic, $P\bar{1}$, a = 9.7578(2) Å, b = 11.2552(3) Å, c = 11.8308(3) Å, α = 115.403(2), β = 97.181(2), γ = 106.900(2), V = 1075.12 Å^3, Z: 1 Z': 0, R = 4.93. ORTEP representation is shown (Fig. 6).

***N*-{4-[4-({6*H*,7*H*,8*H*,9*H*,10*H*-Cyclohepta[*b*]quinolin-11-yl}-amino)phenyl]phenyl}-6*H*,7*H*,8*H*,9*H*,10*H*-cyclohepta[*b*]quinolin-11-amine (22).** This compound was obtained using the same procedure as that for compound **14**. The following quantities of reagents were used: 247.2 mg (1.06 mmol) of compound **7** and 96.9 mg (0.53 mmol) of compound **10**. Compound **22** was obtained as a yellow solid (502.6 mg, 0.49 mmol, 92%), mp 138–144 °C. ^{1}H NMR (400 MHz, CD_3OD): 8.20 (2H, d, $J_{8,7}$ 8.2), 7.99–7.88 (4H, m), 7.69 (4H, d, $J_{3,2}$ 8.6), 7.62 (2H, t, $J_{7,8} = J_{9,8}$ 8.2), 7.20 (4H, d, $J_{2,3}$ 8.6), 3.35–3.24 (4H, m), 2.90 (4H, t, $J_{16,17}$ 5.2), 1.98–1.86 (8H, m), 1.68–1.58 (4H, m). ^{13}C NMR (100 MHz, CD_3OD): 163.2, 154.8, 144.0, 139.6, 138.9, 135.1, 129.7, 129.2, 126.8, 125.5, 124.1, 122.4, 121.7, 36.7, 33.1, 29.4, 28.5, 27.7. Elemental analysis: calc. for $C_{40}H_{38}N_4{\cdot}4C_2HO_2F_3$: C, 55.93; H, 4.11; N, 5.44; found: C, 56.90; H, 3.29; N, 5.69. HRMS (ESI) calc. for $C_{40}H_{38}N_4$ $[M + H]^+$: 575.3175, found: 575.3061.

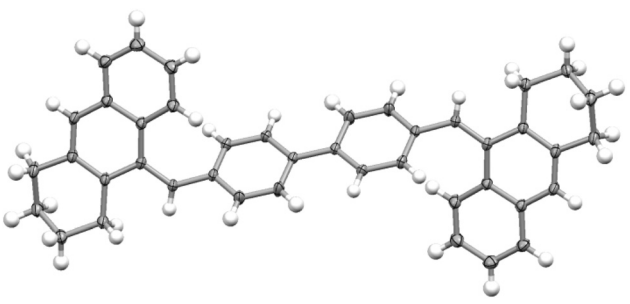

Fig. 6 ORTEP representation of the X-ray crystal structure of compound **21**. The displacement of the ellipsoids is drawn at 50% probability.

***N*^{1},*N*^{5}-Bis(2,3-dihydro-1*H*-cyclopenta[*b*]quinolin-9-yl)naphthalene-1,5-diamine (23).** This compound was obtained using the same procedure as that for compound **14**. The following quantities of reagents were used: 206.2 mg (1.01 mmol) of compound **5** and 78.8 mg (0.5 mmol) of compound **11**. Compound **23** was obtained as a dark green solid (303.6 mg, 0.32 mmol, 64%), which decomposes at 310 °C. ^{1}H NMR (400 MHz, CD_3OD): 8.63 (2H, d, $J_{9,8}$ 7.0), 8.15 (2H, d, $J_{10,11}$ 7.0), 8.00 (2H, t, $J_{9,10} = J_{11,10}$ 7.0), 7.91 (2H, t, $J_{8,9} = J_{10,9}$ 7.0), 7.80 (2H, t, $J_{2,3} = J_{4,3}$ 8.0), 7.74–7.63 (4H, m), 3.20–3.14 (4H, m), 2.25–1.96 (4H, m), 1.89–1.65 (4H, m). ^{13}C NMR (50 MHz, CF_3CO_2D): 164.9, 154.3, 142.7, 140.2, 139.7, 136.0, 130.1, 130.0, 129.3, 124.5, 122.0, 120.1, 119.8, 119.5, 34.1, 33.4, 24.8. Elemental analysis: calc. for $C_{34}H_{28}N_4{\cdot}2C_2HO_2F_3{\cdot}2H_2O$ C, 60.32; H, 4.53; N, 7.40; found: C, 59.69; H, 2.91; N, 8.48. HRMS (ESI) calc. for $C_{34}H_{28}N_4$ $[M + H]^+$: 493.2922, found: 493.2452.

***N*^{1},*N*^{5}-Bis(5,6,7,8-tetrahydroacridin-9-yl)naphthalene-1,5-diamine (24).** This compound was obtained using the same procedure as that for compound **14**. The following quantities were used: 208.2 mg (0.96 mmol) of compound **6** and 75.6 mg (0.48 mmol) of compound **11**. Compound **24** was obtained as a dark brown solid (196.9 mg, 0.2 mmol, 42%), which decomposes at 280 °C. ^{1}H NMR (400 MHz, CD_3OD): 8.09 (2H, d, $J_{9,8}$ 8.2), 7.98 (2H, d, $J_{10,11}$ 8.2), 7.81 (2H, t, $J_{9,10} = J_{11,10}$ 8.2), 7.73 (2H, d, $J_{3,4}$ 8.2), 7.65 (2H, t, $J_{8,9} = J_{10,9}$ 8.2), 7.60–7.52 (2H, m), 7.29 (2H, t, $J_{2,3} = J_{4,3}$ 8.2), 3.23–3.10 (4H, m), 2.64–2.45 (4H, m), 2.11–1.66 (8H, m). ^{13}C NMR (100 MHz, CD_3OD): 155.4, 153.5, 138.3, 130.8, 127.1, 126.9, 126.2, 126.0, 124.7, 124.2, 120.9, 120.0, 119.3, 117.6, 28.5, 24.8, 21.7, 20.6. Elemental analysis: calc. for $C_{36}H_{32}N_4{\cdot}3C_2HO_2F_3{\cdot}H_2O$: C, 57.27; H, 4.23; N, 6.36; found: C, 57.74; H, 3.64; N, 7.82.

***N*^{1},*N*^{5}-Bis(7,8,9,10-tetrahydro-6*H*-cyclohepta[*b*]quinolin-11-yl)-naphthalene-1,5-diamine (25).** This compound was obtained using the same procedure as that for compound **14**. The following quantities of reagents were used: 213.7 mg (0.92 mmol) of compound **7** and 72.5 mg (0.46 mmol) of compound **11**. Compound **25** was obtained as a dark brown solid (263.5 mg, 0.26 mmol, 57%), which decomposes at 252 °C. ^{1}H NMR (400 MHz, CD_3OD): 8.14 (2H, d, $J_{3,2}$ 8.6), 8.04–7.86 (6H, m), 7.61–7.49 (4H, m), 7.42–7.28 (2H, m), 3.29–3.23 (4H, m), 2.69 (4H, t, $J_{17,18}$ 5.4), 1.94–1.74 (8H, m), 1.55–1.14 (4H, m). ^{13}C NMR (100 MHz, CD_3OD): 163.1, 156.8, 141.5, 132.2, 129.2, 129.0, 128.1, 126.4, 124.5, 123.6, 123.0, 122.2, 121.7, 121.1, 36.5, 32.9, 28.9, 27.8, 27.7. Elemental analysis: calc. for $C_{38}H_{36}N_4{\cdot}3C_2HO_2F_3{\cdot}H_2O$: C, 58.15; H, 4.55; N, 6.16; found: C, 57.68; H, 3.91; N, 7.82.

***N*-(4-((4-(2,3-Dihydro-1*H*-cyclopenta[*b*]quinolin-9-ylamino)-phenyl)methyl)phenyl)-2,3-dihydro-1*H*-cyclopenta[*b*]quinolin-9-amine (26).** This compound was obtained using the same

procedure as that for compound **14**. The following quantities of reagents were used: 195.0 mg (0.96 mmol) of compound **5** and 94.3 mg (0.48 mmol) of compound **12**. Compound **26** was obtained as a beige solid (436.6 mg, 0.44 mmol, 92%), mp >360 °C. ^{1}H NMR (400 MHz, CD_3OD): 8.43 (2H, d, $J_{9,8}$ 7.8), 7.93 (2H, t, $J_{11,10} = J_{9,10}$ 7.8), 7.85 (2H, d, $J_{10,11}$ 7.8), 7.71 (2H, t, $J_{8,9} = J_{10,9}$ 7.8), 7.38 (4H, d, $J_{4,3}$ 8.3), 7.29 (4H, d, $J_{3,4}$ 8.3), 4.16 (2H, s), 3.19 (4H, t, $J_{15,14}$ 7.6), 2.37 (4H, t, $J_{15,16}$ 7.6), 2.08 (4H, qui, $J_{16,15} = J_{14,15}$ 7.6). ^{13}C NMR (100 MHz, CD_3OD): 164.5, 153.8, 142.8, 140.3, 139.1, 135.0, 131.4, 128.8, 128.7, 125.4, 121.6, 120.3, 118.5, 42.6, 33.6, 33.3, 24.9. Elemental analysis: calc. for $C_{37}H_{32}N_4 \cdot 3C_2HO_2F_3 \cdot H_2O$: C, 57.85; H, 4.23; N, 6.28; found: C, 58.26; H, 4.18; N, 7.26.

***N*-(4-((4-(5,6,7,8-Tetrahydroacridin-9-ylamino)phenyl)methyl)-phenyl)-5,6,7,8-tetrahydroacridin-9-amine (27).** This compound was obtained using the same procedure as that for compound **15**. The following quantities of reagents were used: 197.5 mg (0.91 mmol) of compound **6** and 89.9 mg (0.45 mmol) of compound **12**. Compound **27** was obtained as an orange solid (248.1 mg, 0.39 mmol, 87%), mp 286–292 °C. ^{1}H NMR (400 MHz, CD_3OD): 7.90–7.84 (6H, m), 7.39 (2H, t, $J_{8,9} = J_{10,9}$ 8.0), 7.32 (4H, d, $J_{4,3}$ 8.0), 7.17 (4H, d, $J_{3,4}$ 8.0), 4.09 (2H, s), 3.15 (4H, t, $J_{15,14}$ 6.0), 2.59 (4H, t, $J_{16,17}$ 8.0), 1.99–1.89 (8H, m). ^{13}C NMR (100 MHz, CD_3OD): 155.4, 154.4, 140.7, 139.6, 134.3, 131.2, 127.0, 126.5, 125.6, 121.0, 120.5, 111.1, 42.0, 32.4, 29.8, 26.3, 23.0, 22.0. Elemental analysis: calc. for $C_{39}H_{36}N_4 \cdot 3HCl \cdot H_2O$: C, 68.07; H, 6.04; N, 8.14; found: C, 68.33; H, 5.76; N, 8.28. HRMS (ESI) calc. for $[C_{39}H_{36}N_4 + H]^+$: 561.3018, found: 561.3596.

***N*-(4-((4-(7,8,9,10-Tetrahydro-6*H*-cyclohepta[*b*]quinolin-11-ylamino)phenyl)methyl)phenyl)-7,8,9,10-tetrahydro-6*H*-cyclohepta[*b*]quinolin-11-amine (28).** This compound was obtained using the same procedure as that for compound **15**. The following quantities of reagents were used: 195.1 mg (0.84 mmol) of compound **7** and 82.8 mg (0.42 mmol) of compound **12**. Compound **28** was obtained as a beige solid (250.1 mg, 0.38 mmol, 90%), mp 246–251 °C. ^{1}H NMR (400 MHz, CD_3OD): 8.14 (2H, d, $J_{9,8}$ 8.3), 7.91 (2H, t, $J_{11,10} = J_{9,10}$ 8.3), 7.89 (2H, d, $J_{10,11}$ 8.3), 7.56 (2H, t, $J_{8,9} = J_{10,9}$ 8.3), 7.25 (4H, d, $J_{4,3}$ 8.6), 7.10 (4H, d, J_{34} 8.6), 4.02 (2H, s), 3.28–3.22 (4H, m), 2.82 (4H, t, $J_{17,18}$ 5.3), 1.93–1.82 (8H, m), 1.60–1.50 (4H, m). ^{13}C NMR (100 MHz, CD_3OD): 162.9, 155.1, 142.6, 140.9, 139.5, 135.0, 132.0, 128.9, 126.7, 124.5, 122.0, 121.6, 42.4, 36.6, 33.1, 29.2, 28.4, 27.7. Elemental analysis: calc. for $C_{41}H_{40}N_4 \cdot 4HCl \cdot 2H_2O$: C, 63.9; H, 6.28; N, 7.27; found: C, 64.0; H, 4.41; N, 6.94.

***N*-(4-(2-(4-(2,3-Dihydro-1*H*-cyclopenta[*b*]quinolin-9-ylamino)-phenyl)ethyl)phenyl)-2,3-dihydro-1*H*-cyclopenta[*b*]quinolin-9-amine (29).** This compound was obtained using the same procedure as that for compound **14**. The following quantities of reagents were used: 189.5 mg (0.93 mmol) of compound **5** and 97.8 mg (0.46 mmol) of compound **13**. Compound **29** was obtained as a light gray solid (442.8 mg, 0.44 mmol, 96%). ^{1}H NMR (400 MHz, CD_3OD): 8.41 (2H, d, $J_{9,8}$ 8.0), 7.92 (2H, t, $J_{11,10} = J_{9,10}$ 8.0), 7.84 (2H, d, $J_{10,11}$ 8.0), 7.70 (2H, t, $J_{8,9} = J_{10,9}$ 8.0), 7.28 (4H, d, $J_{4,3}$ 8.3), 7.23 (4H, d, $J_{3,4}$ 8.3), 3.17 (4H, t, $J_{15,14}$ 7.7), 3.07 (4H, s), 2.34 (4H, t, $J_{15,16}$ 7.5), 2.07 (4H, qui, $J_{16,15} = J_{14,15}$ 7.5). ^{13}C NMR (100 MHz, CD_3OD): 164.4, 153.8, 143.3, 140.3, 138.8, 134.9, 131.3, 128.8, 128.5, 125.3, 121.6, 120.2, 118.3, 39.3, 33.6, 33.3, 24.8. Elemental analysis: calc. for $C_{38}H_{34}N_4 \cdot 3C_2HO_2F_3 \cdot H_2O$: C, 58.28; H, 4.34; N, 6.18; found: C, 58.41; H, 3.01; N, 7.13. HRMS (ESI) calc. for $C_{38}H_{34}N_4$ $[M + H]^+$: 547.2862, found: 547.3234.

***N*-(4-(2-(4-(5,6,7,8-Tetrahydroacridin-9-ylamino)phenyl)ethyl)-phenyl)-5,6,7,8-tetrahydroacridin-9-amine (30).** This compound was obtained using the same procedure as that for compound **14**. The following quantities of reagents were used: 188.7 mg (0.87 mmol) of compound **6** and 90.0 mg (0.42 mmol) of compound **13**. Compound **30** was obtained as a yellow solid (368.0 mg, 0.36 mmol, 85%). ^{1}H NMR (400 MHz, CD_3OD): 7.88–7.73 (6H, m), 7.37 (2H, t, $J_{8,9} = J_{10,9}$ 7.7), 7.23 (4H, d, $J_{4,3}$ 8.3), 7.13 (4H, d, $J_{3,4}$ 8.3), 3.12 (4H, t, $J_{15,14}$ 6.0), 3.03 (4H, s), 2.57 (4H, t, $J_{16,17}$ 6.0), 1.99–1.84 (8H, m). ^{13}C NMR (100 MHz, CD_3OD): 156.2, 155.2, 142.3, 141.1, 140.3, 135.0, 131.8, 127.6, 127.2, 126.2, 121.2, 119.6, 117.4, 39.3, 30.4, 26.9, 23.7, 22.7. Elemental analysis: calc. for $C_{40}H_{38}N_4 \cdot 3C_2HO_2F_3 \cdot H_2O$: C, 59.10; H, 4.64; N, 5.99; found: C, 59.06; H, 3.01; N, 7.13. HRMS (ESI) calc. for $C_{40}H_{38}N_4$ $[M + H]^+$: 575.3175, found: 575.3698.

***N*-(4-(2-(4-(7,8,9,10-Tetrahydro-6*H*-cyclohepta[*b*]quinolin-11-ylamino)phenyl)ethyl)phenyl)-7,8,9,10-tetrahydro-6*H*-cyclohepta-[*b*]quinolin-11-amine (31).** This compound was obtained using the same procedure as that for compound **14**. The following quantities of reagents were used: 195.3 mg (0.84 mmol) of compound **7** and 88.3 mg (0.42 mmol) of compound **13**. Compound **31** was obtained as an orange solid (244.6 mg, 0.23 mmol, 55%). ^{1}H NMR (400 MHz, CD_3OD): 8.11 (2H, d, $J_{9,8}$ 8.6), 7.91 (2H, t, $J_{11,10} = J_{9,10}$ 8.0), 7.86 (2H, d, $J_{10,11}$ 8.5), 7.55 (2H, t, $J_{8,9} = J_{10,9}$ 7.7), 7.20 (4H, d, $J_{4,3}$ 8.3), 7.07 (4H, d, J_{34} 8.3), 3.27–3.18 (4H, m), 2.98 (4H, s), 2.81 (4H, t, $J_{17,18}$ 5.2), 1.94–1.81 (8H, m), 1.60–1.49 (4H, m). ^{13}C NMR (100 MHz, CD_3OD): 162.7, 155.2, 142.3, 141.3, 139.5, 135.0, 131.9, 128.8, 126.7, 124.5, 124.1, 121.8, 121.6, 39.2 36.5, 33.1, 29.2, 28.5, 27.7. Elemental analysis: calc. for $C_{42}H_{42}N_4 \cdot 2C_2HO_2F_3 \cdot 3H_2O$: C, 62.44; H, 5.70; N, 6.36; found: C, 62.40; H, 4.65; N, 7.46.

Concentration–response curves and IC_{50} determination

The concentration–response curves for the determination of IC_{50} values were obtained using Ellman's methodology.[98] The enzymes hAChE (human acetylcholinesterase, recombinant, expressed in HEK 293 cells, lyophilized powder, ≥1.500 units per mg protein), hBChE (human, recombinant, expressed in goat, ≥500 units per mg protein), *Ee*AChE (*Electrophorus electricus*, Type VI-S, lyophilized powder, 200–1.000 units per mg protein) and eqBChE (from equine serum, lyophilized powder, ≥900 units per mg protein) were purchased from Sigma-Aldrich. The chemicals DTNB (5,5′-dithio bis(2-nitrobenzoic acid)), ATChI (acetylthiocholine iodide) and BTChI (*S*-butyrylthiocholine iodide) were also purchased from Sigma-Aldrich. Enzyme activity was performed in phosphate buffer pH 8.0 containing 0.3 mM DTNB, either ATChI or BTChI at 0.3 mM and each enzyme (individually) at 0.1 U mL^{-1} in the presence

or absence of tacrine or tacrine dimers (10^{-3} to 10^{-10} M). Reactions were stopped after 2.5 min of incubation at 25 °C and the absorbance was measured at 412 nm. All experiments were done at least in triplicate and the percentage of inhibition exhibited by each synthesized compound was calculated using eqn (1), where ΔA_i refers to the change in absorbance in the presence of an inhibitor, and ΔA represents the change in the average catalysis absorbance without an inhibitor.

$$I(\%) = \left(1 - \frac{\Delta A_i}{\Delta A}\right) \times 100 \quad (1)$$

The concentration–response curves were constructed by sigmoidal regression from the data plot of % inhibition as a function of the log [inhibitor] with the aid of the Origin 6.0 software package (Microcal Software, Inc., Northampton, MA 01060, USA). The IC_{50} values were determined from the concentration–response curves and correspond to the concentration of the inhibitor necessary to inhibit the enzyme activity by 50%.[45]

Kinetic assays

For the kinetic studies, the concentration of substrates varied from 10^{-3} to 10^{-10} M while four different concentrations near the IC_{50} were tested for tacrine or tacrine dimers. These experiments were conducted at least in triplicate. The velocity of catalysis was determined according to eqn (2), where ΔA refers to the absorbance variation of the reference substance at a given wavelength as a function of the reaction time, and 13 600 refers to the molar absorptivity coefficient of the anion 5-thio-2-nitro-benzoic acid.

$$v\left(\frac{\text{mol}}{\text{L min}^{-1}}\right) = \frac{\Delta A}{\text{min}}/13\,600 \quad (2)$$

The kinetic profile was assessed using eqn (3), where v_o is the initial velocity, V_{max} is the maximum velocity for the enzyme, [S] is the substrate concentration, [I] is the inhibitor concentration, α is the factor related to the change in the reaction constant caused by the inhibitor, and K_m is the Michaelis–Menten constant.[28,35,46,56,99,100]

$$v_o = \frac{V_{max}[S]}{[S]\left(1 + \frac{[I]}{\alpha K_i}\right) + K_m\left(1 + \frac{[I]}{K_i}\right)} \quad (3)$$

The slope method was used to determine the inhibitory constants.[50] The α values were obtained from Dixon plots.[83] The slope and $1/V_{max}$ values were determined from Lineweaver–Burk plots.[101]

Molecular modeling

The calculation of minimal energy and the estimation of pK_a values for the synthesized molecules were carried out using the software Marvin Sketch 5.8.0 (Fine Builder) (ChemAxon) and DS Visualizer 3.1 (Accelrys Inc.) and the AutoDock Tools package (ADT 1.5.4).[102] X-ray structures available in the Protein Data Bank (http://www.rcsb.org) were used as follows: 3LII (hAChE),[103] 1B41 (hAChE),[104] 4EY4 (hAChE),[61] 1EA5 (*Tc*AChE),[67] 1ACJ (*Tc*AChE),[69] 2CKM (*Tc*AChE),[35] 1C2O (*Ee*AChE),[62] and 1P0I (hBChE).[76] The UniProtAC Q9N1N9 (eqBChE) program was used to build the homology model of eqBChE.[77–79] The software SwissPDB Viewer 4.0.1[79] was used for removing water molecules and obtaining the final protein structure. The software AutoDock Vina[105] was adopted to perform molecular docking, in which the receptor structure was defined as rigid, and the grid dimensions were 74 Å, 52 Å and 78 Å for the axes *X*, *Y* and *Z*, respectively, in the catalytic gorge region with a resolution of 0.375 Å. The visualization studies were conducted with PyMOL Viewer™ 1.3.[106]

Acknowledgements

We are grateful to Dr I.S. Lula, BSc. M.A. Perdigão de Assis, Dr L.A. do Nascimento and MSc. L.H.R. dos Santos for the technical assistance with NMR, CHN, HRMS and X-ray analyses, respectively. This work was supported by Fundação de Amparo à Pesquisa do Estado de Minas Gerais (FAPEMIG) and Conselho Nacional de Desenvolvimento Científico e Tecnológico (CNPq). R.A.N. de Aquino was supported by a scholarship from Centro Federal de Educação Tecnológica de Minas Gerais (CEFET-MG). L.V. Modolo, R.B. Alves and A. de Fátima are supported by research fellowships from CNPq. A. de Fátima also benefited from financial support provided by the Pró-Reitoria de Pesquisa da UFMG.

References

1 S. Darvesh, D. A. Hopkins and C. Geula, *Nat. Rev.*, 2003, **4**, 131–138.
2 C. Mattes, R. Bradley, E. Slaughter and S. Browne, *Life Sci.*, 1996, **58**, 257–261.
3 T. D. Shori and H. Soininen, *Curr. Alzheimer Res.*, 2010, **7**, 67–73.
4 N. H. Greig, T. Utsuki, D. K. Ingram, Y. Wang, G. Pepeu, C. Scali, Q. S. Yu, S. J. Mamczarz and H. W. Holloway, *Proc. Natl. Acad. Sci. U. S. A.*, 2005, **102**, 17213–17218.
5 M. M. Mesulam, A. Guillozeta, P. Shaw, A. Levey, E. G. Duysen and O. Lockridge, *Neuroscience*, 2002, **110**, 627–639.
6 T. Lee, D. Lee, Y. Lee and Y. D. Gong, *J. Comb. Chem.*, 2010, **12**, 95–99.
7 C. M. Spencer and S. Noble, *Drug Aging*, 1998, **13**, 391–411.
8 I. McKeith, T. D. Ser, P. Spano, M. Emre, K. Wesnes, R. Anand, A. C. Sain, R. Ferrara and R. Spiegel, *Lancet*, 2000, **356**, 2031–2036.
9 E. A. Werber and J. M. Rabey, *J. Neural. Transm.*, 2001, **108**, 1319–1325.
10 V. Kumar, R. Anand, J. Messina, R. Hartma and J. Veach, *Eur. J. Neurol.*, 2000, **7**, 159–169.
11 C. A. Masanic, M. T. Bayey, R. V. Reekum and M. Simard, *Arch. Phys. Med. Rehabil.*, 2001, **82**, 896–901.

12 J. Porcel and X. Montalban, *J. Neurol. Sci.*, 2006, **245**, 177–181.
13 T. Hikida, Y. Kitabatake, I. Pastan and S. Nakanishi, *Proc. Natl. Acad. Sci. U. S. A.*, 2003, **100**, 6169–6173.
14 K. Musilek, R. Pavlikova, J. Marek, M. Komloova, O. Holas, M. Hrabinova, M. Pohanka, V. Dohnal, M. Dolezal, F. G. Moore and K. Kuca, *J. Enzyme Inhib. Med. Chem.*, 2011, **26**, 245–253.
15 F. Bergmann, I. B. Wilson and D. Nachmansohn, *Biochim. Biophys. Acta*, 1950, **6**, 217–224.
16 L. Austin and W. K. Berry, *Biochem. J.*, 1953, **54**, 695–700.
17 W. Li, M. Mak, H. Jiang, Q. Wang, Y. P. Pang, K. Chen and Y. Han, *Neurotherapeutics*, 2009, **6**, 187–201.
18 H. Fu, J. Dou, W. Li, W. Cui, S. Mak, Q. Hu, J. Luo, C. S. C. Lam, Y. P. Pang, M. B. H. Youdim and Y. Han, *Eur. J. Pharmacol.*, 2009, **623**, 14–21.
19 M. L. Bolognesi, E. Simoni, M. Rosini, A. Minarini, V. Tumiatti and C. Melchiorre, *Curr. Top. Med. Chem.*, 2011, **11**, 2797–2806.
20 A. Albert and W. J. Gledhill, *J. Soc. Chem. Ind.*, 1945, **64**, 169–172.
21 F. H. Shaw and G. A. Bentley, *Acta Chem. Scand.*, 1961, **15**, 1386–1390.
22 E. Heilbronn, *Acta Chem. Scand.*, 1961, **15**, 1386–1390.
23 K. L. Davis and P. Powchik, *Lancet*, 1995, **345**, 625–630.
24 P. B. Watkins, H. J. Zimmerman, M. J. Knapp, S. I. Gracon and L. W. Lewis, *JAMA*, 1994, **271**, 992–998.
25 J. Patocka, D. Jun and K. Kuca, *Curr. Drug. Metab.*, 2008, **9**, 332–335.
26 R. A. N. de Aquino, L. V. Modolo, R. B. Alves and A. de Fátima, *Curr. Drug. Targets*, 2013, **14**, 378–397.
27 G. Pastorin, S. Marchesan, J. Hoebeke, T. Da Ros, L. E. Sabatier, J. P. Briand and M. P. A. Bianco, *Org. Biomol. Chem.*, 2006, **4**, 2556–2562.
28 Y. P. Pang, P. Quiram, T. Jelacic, F. Hong and S. Brimijoin, *J. Biol. Chem.*, 1996, **271**, 23646–23649.
29 M. L. Bolognesi, A. Cavalli, L. Valgimigli, M. Bartolini, M. Rosini, V. Andrisano, M. Recanatini and C. Melchiorre, *J. Med. Chem.*, 2007, **50**, 6446–6449.
30 P. E. Cramer, J. R. Cirrito, D. W. Wesson, C. Y. D. Lee, J. C. Karlo, A. E. Zinn, B. T. Casali, J. L. Restivo, W. D. Goebel, M. J. James, K. R. Brunden, D. A. Wilson and G. E. Landreth, *Science*, 2012, **335**, 1503–1506.
31 B. Winblad, N. Andreasen, L. Minthon, A. Floesser, G. Imbert, T. Dumortier, R. P. Maguire, K. Blennow, J. Lundmark, M. Staufenbiel, J. M. Orgogozo and A. Graf, *Lancet*, 2012, **11**, 597–604.
32 J. Stöhr, J. C. Watts, Z. L. Mensinger, A. Oehler, S. K. Grillo, S. J. DeArmond, S. B. Prusiner and K. Giles, *Proc. Natl. Acad. Sci. U. S. A.*, 2012, **109**, 11025–11030.
33 M. Ouberai, K. Brannstrom, M. Vestling, A. Olofsson, P. Dumy, S. Chierici and J. Garcia, *Org. Biomol. Chem.*, 2011, **9**, 1140–1147.
34 P. W. Elsinghorst, W. Härtig, S. Goldhammer, J. Grosche and M. Gütschow, *Org. Biomol. Chem.*, 2009, **7**, 3940–3946.
35 E. H. Rydberg, B. Brumshtein, H. M. Greenblatt, D. M. Wong, D. Shaya, L. D. Williams, P. R. Carlier, Y. Pang, I. Silman and J. L. Sussman, *J. Med. Chem.*, 2006, **49**, 5491–5500.
36 N. C. Inestrosa, A. Alvarez, C. A. Pérez, R. D. Moreno, M. Vicente, C. Linker, O. I. Casanueva, C. Soto and J. Garrido, *Neuron*, 1996, **16**, 881–891.
37 M. Recanatini and P. Valenti, *Curr. Pharm. Des.*, 2004, **10**, 3157–3166.
38 S. Butini, G. Campiani, M. Borriello, S. Gemma, A. Panico, M. Persico, B. Catalanotti, S. Ros, M. Brindisi, M. Agnusdei, I. Fiorini, V. Nacci, E. Novellino, T. Belinskaya, A. Saxena and C. Fattorusso, *J. Med. Chem.*, 2008, **51**, 3154–3170.
39 W. Jahnke, R. M. Grotzfeld, X. Pellé, A. Strauss, G. Fendrich, S. W. C. Jacob, S. Cotesta, D. Fabbro, P. Furet, J. Mestan and A. L. Marzinzik, *J. Am. Chem. Soc.*, 2010, **132**, 7043–7048.
40 F. H. Allen, J. E. Davies, J. J. Galloy, O. Johson, O. Kennard, C. F. Macrae, E. M. Mitchell, G. F. Mitchell, J. M. Smith and D. G. Watson, *J. Chem. Inf. Comput. Sci.*, 1991, **31**, 187–204.
41 M. K. Hu and C. F. Lu, *Tetrahedron Lett.*, 2000, **41**, 1815–1818.
42 F. B. Hasan, S. G. Cohen and J. B. Cohen, *J. Biol. Chem.*, 1980, **255**, 3898–3904.
43 C. Sotriffer, G. Klebe, M. Stahl and H. J. Bohm, *Docking and Scoring Functions and Virtual Screening in Burger's Medicinal Chemistry and Drug Discovery*, John Wiley and Sons Inc., New York, 2003, vol. 1, pp. 281–332.
44 G. Koellner, T. Steiner, C. B. Millard, I. Silman and J. L. Sussman, *J. Mol. Biol.*, 2002, **320**, 721–725.
45 P. R. Carlier, Y. F. Han, E. S. H. Chow, C. P. L. Li, H. Wang, T. X. Lieu, H. S. Wong and Y. Pang, *Bioorg. Med. Chem.*, 1999, **7**, 351–357.
46 R. A. Copeland, *Enzymes: A Practical Introduction to Structure, Mechanism, and Data Analysis*, John Wiley and Sons Inc., New York, 2000.
47 R. B. G. Ravelli, M. L. Raves, Z. Ren, D. Bourgeois, M. Roth, J. Kroon, I. Silman and J. L. Sussman, *Acta Crystallogr., Sect. D: Biol. Crystallogr.*, 1998, **54**, 1359–1366.
48 S. Senapati, J. M. Bui and J. A. McCammon, *J. Med. Chem.*, 2005, **48**, 8155–8162.
49 J. L. Taylor, R. T. Mayer and C. M. Himel, *Mol. Pharmacol.*, 1994, **45**, 74–83.
50 I. H. Segel, *Enzyme Kinetics*, John Wiley and Sons Inc., New York, 1975.
51 F. Bergmann and R. Segal, *Biochem. J.*, 1954, **58**, 692–698.
52 P. Taylor and S. Lappi, *Biochemistry*, 1975, **14**, 1989–1997.
53 H. M. Greenblatt, G. Kryger, T. Lewis, I. Silman and J. Sussman, *FEBS Lett.*, 1999, **463**, 321–326.
54 M. C. Desai, P. F. Thadeio, C. A. Lipinski, D. R. Liston, R. W. Spencer and I. H. Williams, *Biorg. Med. Chem. Lett.*, 1991, **1**, 411–414.
55 G. M. Steinberg, M. L. Mednick, J. Maddox, R. Rice and J. Cramer, *J. Med. Chem.*, 1975, **18**, 1056–1061.

56 L. Huang, T. Su, W. Shan, Z. Luo, Y. Sun, F. He and X. Li, *Bioorg. Med. Chem.*, 2012, **20**, 3038–3048.
57 J. L. Sussman, M. Harel and I. Silman, *Chem.-Biol. Interact.*, 1993, **87**, 187–197.
58 D. A. Dougherty and D. A. Stauffer, *Science*, 1990, **250**, 1558–1560.
59 J. P. Colletier, B. Sanson, F. Nachon, E. Gabellieri, C. Fattorusso, G. Campiani and M. Weik, *J. Am. Chem. Soc.*, 2006, **128**, 4526–4527.
60 Y. Bourne, H. C. Kolb, Z. Radić, K. B. Sharpless, P. Taylor and P. Marchot, *Proc. Natl. Acad. Sci. U. S. A.*, 2004, **101**, 1449–1454.
61 J. Cheung, M. J. Rudolph, F. Burshteyn, M. S. Cassidy, E. N. Gary, J. Love, M. C. Franklin and J. J. Height, *J. Med. Chem.*, 2012, **55**, 10282–10286.
62 Y. Bourne, J. Grassi, P. E. Bougis and P. Marchot, *J. Biol. Chem.*, 1999, **274**, 30370–30376.
63 M. K. Gilson, T. P. Straatsma, J. A. McCammon, D. R. Ripoll, C. H. Faerman, P. H. Axelsen, I. Silman and J. L. Sussman, *Science*, 1994, **263**, 1276–1278.
64 C. D. Personeni, P. D. Bentley, R. J. Fletcher, A. Kinkaid, G. Kryger, B. Pirard, A. Taylor, R. Taylor, J. Taylor, R. Viner, I. Silman, J. L. Sussman, H. M. Greenblatt and T. Lewis, *J. Med. Chem.*, 2001, **44**, 3203–3215.
65 C. Kronman, A. Ordentlich, D. Barak, B. Velan and A. Shafferman, *J. Biol. Chem.*, 1994, **269**, 27819–27822.
66 H. M. Greenblatt, H. Dvir, I. Silman and J. L. Sussman, *J. Mol. Neurosci.*, 2003, **20**, 369–383.
67 H. Dvir, H. L. Jiang, D. M. Wong, M. Harel, M. Chetrit, X. C. He, G. Y. Jin, G. L. Yu, X. C. Tang, I. Silman, D. L. Bai and J. L. Sussman, *Biochemistry*, 2002, **41**, 10810–10818.
68 M. Harel, J. L. Sussman, E. Krejci, S. Bon, P. Chanal, J. Massoulié and I. Silman, *Proc. Natl. Acad. Sci. U. S. A.*, 1992, **89**, 10827–10831.
69 M. Harel, I. Schalk, L. E. Sabatier, F. Bouet, M. Goeldner, C. Hirth, P. H. Axelsen, I. Silman and J. L. Sussman, *Proc. Natl. Acad. Sci. U. S. A.*, 1993, **90**, 9031–9035.
70 G. Koellner, G. Kryger, C. B. Millard, I. Silman, J. L. Sussman and T. Steiner, *J. Mol. Biol.*, 2000, **296**, 713–735.
71 G. Campiani, C. Fattorusso, S. Butini, A. Gaeta, M. Agnusdei, S. Gemma, M. Persico, B. Catalanotti, L. Savini, V. Nacci, E. Novellino, H. W. Holloway, N. H. Greig, T. Belinskaya, J. M. Fedorko and A. Saxena, *J. Med. Chem.*, 2005, **48**, 1919–1929.
72 M. L. Bolognesi, M. Bartolini, F. Mancini, G. Chiriano, L. Ceccarini, M. Rosini, A. Milelli, V. Tumiatti, V. Andrisano and C. Melchiorre, *ChemMedChem*, 2010, **5**, 1215–1220.
73 P. Y. Lam, P. K. Jadhav, C. J. Eyermann, C. N. Hodge, Y. Ru, L. T. Bacheler, J. L. Meek, M. J. Otto, M. M. Rayner, Y. N. Wong, C. H. Chang, P. C. Weber, D. A. Jackson, T. R. Sharpe and S. E. Viitanen, *Science*, 1994, **263**, 380–384.
74 J. C. Basurto, J. E. Raya, M. G. May, L. M. E. Fonseca, I. V. Alcántara and J. T. Ferrara, *J. Enzyme Inhib. Med. Chem.*, 2006, **21**, 133–138.
75 N. Morel, S. Bon, H. M. Greenblatt, D. V. Belle, S. J. Wodak, J. L. Sussman, J. Massoulié and I. Silman, *Mol. Pharmacol.*, 1999, **55**, 982–992.
76 Y. Nicolet, O. Lockridge, P. Masson, J. C. F. Camps and F. Nachon, *J. Biol. Chem.*, 2003, **278**, 41141–41147.
77 K. Arnold, L. Bordoli, J. Kopp and T. Schwede, *Bioinformatics*, 2006, **22**, 195–201.
78 T. Schwede, J. Kopp, N. Guex and M. C. Peitsch, *Nucleic Acids Res.*, 2003, **31**, 3381–3385.
79 N. Guex and M. C. Peitsch, *Electrophoresis*, 1997, **18**, 2714–2723.
80 H. Neurath, *J. Am. Chem. Soc.*, 1943, **65**, 2039–2041.
81 J. Korabecny, O. Holas, K. Musilek, M. Pohanka, V. Opletalova, V. Dohnal and K. Kuca, *Lett. Org. Chem.*, 2010, **7**, 327–331.
82 C. M. G. Tanarro and M. Gütschow, *J. Enzyme Inhib. Med. Chem.*, 2011, **26**, 350–358.
83 M. Dixon, *Biochem. J.*, 1953, **55**, 170.
84 R. M. Krupka, *Biochemistry*, 1964, **3**, 1749–1754.
85 J. Debord, L. Merle, J. C. Bollinger and T. Dantoine, *J. Enzyme Inhib. Med. Chem.*, 2002, **17**, 197–202.
86 T. Szegletes, W. D. Mallender, P. J. Thomas and T. L. Rosenberry, *Biochemistry*, 1999, **38**, 122–133.
87 T. Yonetani and H. Theorell, *Arch. Biochem. Biophys.*, 1964, **106**, 243–251.
88 T. L. Rosenberry and S. A. Bernhard, *Biochemistry*, 1972, **11**, 4308–4432.
89 J. L. Sussman, M. Harel, F. Frolow, C. Oefner, A. Goldman, L. Toker and I. Silman, *Science*, 1991, **253**, 872–879.
90 J. Zhang, F. J. Adrián, W. Jahnke, S. W. C. Jacob, A. G. Li, R. E. Iacob, T. Sim, J. Powers, C. Dierks, F. Sun, G. R. Guo, Q. Ding, B. Okram, Y. Choi, A. Wojciechowski, X. Deng, G. Liu, G. Fendrich, A. Strauss, N. Vajpai, S. Grzesiek, T. Tuntland, Y. Liu, B. Bursulaya, A. Azam, P. W. Manley, J. R. Engen, G. Q. Daley, M. Warmuth and N. S. Gray, *Nature*, 2010, **463**, 501–506.
91 G. B. Cohen, R. Ren and D. Baltimore, *Cell*, 1995, **80**, 237–248.
92 M. R. Arkin and J. A. Wells, *Nat. Rev. Drug Discovery*, 2004, **3**, 301–317.
93 J. Wiesner, Z. Kříž, K. Kuča, D. Jun and J. Koča, *J. Enzyme Inhib. Med. Chem.*, 2010, **25**, 318–322.
94 F. Nachon, L. E. Sabatier, D. Loew, C. Colas, A. V. Dorsselaer and M. Goeldner, *Biochemistry*, 1998, **37**, 10507–10513.
95 J. C. Watson and F. H. C. Crick, *Nature*, 1953, **171**, 737–738.
96 D. D. Boehr, A. R. Farley, G. D. Wright and J. R. Cox, *Chem. Biol.*, 2002, **9**, 1209–1217.
97 X. Cousin, S. Bon, N. Duval, J. Massoulié and C. Bon, *J. Biol. Chem.*, 1996, **271**, 15099–15108.
98 G. L. Ellman, K. D. Courtney, J. R. V. Andres and M. Featherstone, *Biochem. Pharmacol.*, 1961, **7**, 88–95.
99 M. L. Bolognesi, V. Andrisano, M. Bartolini, R. Banzi and C. Melchiorre, *J. Med. Chem.*, 2005, **48**, 24–27.

100 S. Rizzo, A. Bisi, M. Bartolini, F. Mancini, F. Belluti, S. Gobbi, V. Andrisano and A. Rampa, *Eur. J. Med. Chem.*, 2011, **46**, 4336–4343.
101 H. Lineweaver and D. Burk, *J. Am. Chem. Soc.*, 1934, **56**, 658–666.
102 G. M. Morris, D. S. Goodsell, R. S. Halliday, R. Huey, W. E. Hart, R. K. Belew and A. J. Olson, *J. Comput. Chem.*, 1998, **19**, 1639–1662.
103 H. Dvir, I. Silman, M. Harel, T. L. Rosenberry and J. L. Sussman, *Chem.-Biol. Interact.*, 2010, **187**, 10–22.
104 G. Kryger, I. Silman and J. S. Sussman, *Structure Fold. Des.*, 1999, **7**, 297–307.
105 O. Trott and A. J. Olson, *J. Comput. Chem.*, 2010, **31**, 455–461.
106 W. L. DeLano, *The PyMOL Molecular Graphics System on the World Wide Web*, http://www.pymol.org, 2002.